labeled nuclei were commonly observed in the basal, second, and third turns, but very rarely in the apical turn, probably because the OHCs were damaged severely in the lower three turns but mildly to moderately in the apical turn. BrdU-labeled nuclei were located at the regions in which the nuclei of the DCs were normally present, or more apically, at a level normally occupied by the nuclei of the OHCs. The apical portions of BrdU-labeled cells typically demonstrated a DC-like phalangeal process extending to the reticular lamina. BrdU-labeled nuclei were also labeled with p27 and located within the vimentin-positive cytoplasm of the DCs and beneath the cytokeratin-positive expanded apical portion of these cells. These findings indicate that the original sets of cells containing BrdU-labeled nuclei are the DCs.

Nonspecific uptake of BrdU might however have occurred passively in cells with severely damaged DNA, when the cells were in the process of dying. However, several pieces of evidence exclude this possibility. First, administration of KM and EA induced severe damage to the OHCs acutely within a few days, whereas the damage to the IHCs and supporting cells was minimal, as previously observed (West et al. 1973; Yamasoba et al. 2003). Second, animals were killed at least 12 h following the last BrdU injection, which is considered long enough to allow apoptotic cells labeled with BrdU to be removed. Histologically visible stages of the apoptotic process are known to be short, lasting from a few minutes to a maximum of 3 h (Bursch et al. 1990). Although the rate of removal of dead cells may vary in different tissues, previous evaluations in the developing nervous system suggest that this occurs rapidly, within a few hours (Voyvodic et al. 1995; Thomaidou et al. 1997). Third, the number of BrdU-labeled nuclei did not significantly differ between animals given BrdU for 10 days and killed on day 12 and day 31. These findings argue against the BrdU-labeled nuclei observed in the OC having been nonspecifically labeled while being involved in cell death.

The current study revealed that the number of BrdU-labeled nuclei in the OC was small after ototoxic insults. However, we injected BrdU every 12 h. Since BrdU is cleared within approximately 2 h (Matei et al. 2005), BrdU should be injected every 2 h, as shown by Chen et al. (2002), to label all or most proliferating cells. However, given the toxic side-effects of BrdU, such repeated injections would only be tolerable if animals were allowed to survive for a short period. Given the longer survival time required in this study, ethical approval could not be obtained for the repeated higher daily concentrations of BrdU required to capture all cells. Thus, our current assessment is probably conservative, and many more proliferating cells (approximately 6×) might have been observed with more frequent BrdU injections. Even if we only labeled approximately 1/6 of the possible proliferating cells, the proliferation activity of the supporting cells in the OC after hair cell loss still appears limited. In the utricular macula of guinea pig, continuous infusion of cell proliferation marker in vivo for one to several weeks has also revealed that a single injection of gentamicin into the middle ear spaces induces limited cell proliferation (e.g., fewer than 12 labeled cells/utricle; Rubel et al. 1995; Li and Forge 1997). Following gentamicin treatment, a total of 23 ^{3}H-thymidine-labeled supporting cells were observed in four of seven animals (Rubel et al. 1995) and a total of 18 BrdU-labeled nuclei were observed in three of four animals (Li and Forge 1997). These findings suggest that, following ototoxic insults in guinea pigs, cell proliferation may be limited both in the cochleae and in vestibular endorgans.

Cumulative BrdU injection for diverse lengths has revealed that the uptake of BrdU occurs most robustly in the guinea pig OC 3–5 days following hair cell injury. This time window of BrdU uptake is similar to that in chick basilar papilla following insults by systemic aminoglycoside injection; pulse/fix BrdU labeling studies have shown a dramatic increase in BrdU-labeled cells at 3 days following a single systemic injection of gentamicin, and the number of labeled cells decreases rapidly by 5 days following the injection (Bhave et al. 1995; Stone et al. 1999).

When BrdU-labeled nuclei were detected in deafened animals given BrdU for 10 days, closely paired labeled nuclei were observed in approximately one-third of cases. We also found a DC containing BrdU-labeled daughter nuclei, suggesting segregation during mitosis, in an animal given BrdU for 5 days. The presence of the pairs of BrdU-labeled nuclei and a segregating daughter nuclei in the DC suggested that these labeled cells were in S phase at the time of BrdU injection and were able to pass through the G_2 and M phases before analysis. Clusters of more than two labeled cells were not observed, suggesting that the DCs that had taken up BrdU did not go on to divide more than once.

In the deafened animals, BrdU-labeled nuclei in the OC were co-labeled with p27, suggesting that the DCs that had taken up BrdU had exited the cell cycle prior to analysis. It is of importance to understand how these cells can enter the cell cycle, while expressing this negative cell cycle regulator. Fibroblasts still express p27 when they are actively proliferating, although its expression is reduced (Malek et al. 2001). This finding indicates that the presence of p27 in BrdU-positive cells does not mean that they are incapable of cell cycle re-entry. Mice that are heterozygous for the p27 mutation ($p27^{+/-}$), and that contain about 50% of the p27 found in wild-type littermates (Kil et al. 2000) occasionally exhibit supernumerary IHCs (Chen and Segil 1999) but show an increase of BrdU-positive cells in the OC after significant hair cell loss induced by systemic amikacin injection (Kil et al. 2000). These findings suggest that cochlear supporting cells are able to proliferate when p27 is downregulated below a certain level, and that hair cell loss can trigger this proliferation. Positivity for p27 significantly decreases in the DC after topical application of cisplatin to mice; cisplatin kills most OHCs but not DCs (Endo et al. 2002). In view of these observations, we speculate that significant hair cell loss induced by KM and EA may have induced significant downregulation of p27 below a critical level in some DCs, which then enter cell cycle.

Why only a proportion of BrdU-labeled cells has been demonstrated as paired doublets in the damaged OC of guinea pigs, and similarly in the utricular macula of gentamicin-treated guinea pigs in vivo, remains unknown. Rubel et al. (1995) have found only three labeled doublets out of 23 ^{3}H-thymidine labeled supporting cells. Perhaps only a proportion of BrdU-labeled supporting cells might enter G_2 and then M phase after S phase. Another possibility is that some daughter cells may die shortly after division in the inner ear. In the developing or proliferating central or peripheral nervous system, cell death commonly occurs shortly after the replication of DNA or on exiting the cell cycle (Barres et al. 1992; Yaginuma et al. 1996; Thomaidou et al. 1997). Moreover, mice lacking the retinoblastoma gene (*Rb1*), a negative regulator of the cell cycle, show continued proliferation of hair cells and supporting cells, some of which differentiate whereas others degenerate (Mantela et al. 2005).

When we found two paired BrdU-labeled nuclei were found, one was commonly located at a level normally occupied by the nuclei of the DCs and its sister nucleus occurred more apically at a level normally occupied by the nuclei of the OHCs. When paired labeled nuclei were observed in the vimentin-positive cell bodies, typically one was located in the inferior portion of the vimentin-positive cytoplasm of the DCs and second in the superior portion of vimentin-positive cytoplasm of the adjacent sister DCs. These findings suggested that BrdU-labeled nuclei located apically at a level normally occupied by the nuclei of the OHCs had migrated from their original position. Vimentin was faintly stained in the DCs not expressing BrdU but was more strongly stained in the DCs labeled by BrdU, indicative that vimentin synthesis was upregulated in the BrdU-labeled DCs. This is consistent with findings that vimentin is associated with the mitotic apparatus and related to the induction of cellular DNA synthesis or mitosis, and that increases in vimentin synthesis are associated with rapidly growing cells, because of its involvement in the extensive remodeling of cytoskeletal components required for mitosis, migration, and process outgrowth (Baserga 1985; Ferrari et al. 1986). Following hair cell injury, vertical migration of the nuclei labeled with cell proliferation marker has been observed in chick basilar papilla (Stone and Cotanche 1994; Stone and Rubel 2000), in which proliferated sister cell pairs go on to differentiate as a supporting cell and a hair cell, as two supporting cells, or as two hair cells in the chick basilar papilla (Stone and Rubel 2000). We are currently examining whether the DCs that migrate apically after cell division can differentiate to hair cells.

Conceptually, there are several possible ways to attempt the generation of (or introduction of) new hair cells to restore the function of the OC. These include (1) the generation of new cells by mitosis of supporting cells (with some of the progeny differentiating into new hair cells), (2) the conversion of the phenotype of supporting cells to hair cells (with or without mitosis), or (3) the implantation of stem cells or other progenitors that will differentiate to new hair cells. Several lines of research have been conducted for possible interventions to accomplish these goals. For example, in vivo inoculation of adenovirus encoding the *Atoh1* gene into the endolymph of the mature guinea pig cochlea results in the production of new hair cells (Kawamoto et al. 2003; Izumikawa et al. 2005), indicative that nonsensory cells in the mature mammalian cochlea can generate new hair cells after overexpression of genes that are necessary and sufficient for hair cell differentiation. However, in the avian inner ear, the generation of new cells occurs spontaneously, without any therapeutic intervention, via the mitosis of supporting cells: hair cell injury induces supporting cells to become precursors, to re-enter the cell cycle, and to provide daughter cells that become new hair cells (Corwin and Cotanche 1988; Ryals and Rubel 1988; Stone and Cotanche 1994; Bhave et al. 1995; Stone et al. 1999; Stone and Rubel 2000). Our current study demonstrates that at least the first phase of avian hair cell regeneration is indeed possible in the mammal cochlea. A more limited regenerative response has also been observed in the vestibular organs of mammals, in which the reoccurrence of hair cells also reflects supporting cell proliferation (Forge et al. 1993; Rubel et al. 1995; Kuntz and Oesterle 1998). In developing mice lacking p27, a critical factor in cell cycle arrest, cells of the OC continue to proliferate for more than 2 weeks after normal cessation, and supporting cells can generate new hair cells after trauma-induced hair cell loss (Chen and Segil 1999; Raphael 2002), indicating that supporting cells in the mammalian cochlea can differentiate spontaneously into hair cells when they re-enter the cell cycle. The current study has also demonstrated that mature DCs have an albeit limited competence to re-enter the cell cycle and proliferate. If we can enhance cell proliferation of these supporting cells following hair cell injury, we may generate a large enough precursor cell pool to regenerate the mature mammalian cochleae. Presumably, the induction of several mitogenic growth factors that enhance cell proliferation in the mammalian vestibular sensory epithelia or the down-regulation of molecules, such as *p27*, that inhibit cell re-cycling in supporting cells (Kil et al. 2000) may achieve this goal. Interestingly, we have recently observed that inoculation of adenovirus encoding shRNA, which targets p27kip1 mRNA into the deafened guinea pig cochlea, induces supporting cell proliferation and new stereociliary bundles in vivo (unpublished).

Acknowledgements We are grateful to Drs. Josef M. Miller, Joseph E. Hawkins, Yasuya Nomura, and Masato Nakafuku for helpful comments and discussion and to Mr. Yoshiro Mori, Mr. Ko-ichi Miyazawa, Ms. Atsuko Tsuyuzaki, Ms. Yukari Kurasawa, and Dr. Shinichi Ishimoto for technical support.

References

Barres BA, Hart IK, Coles HSR, Burne JF, Voyvodic JT, Richardson WD, Raff MC (1992) Cell death and control of cell survival in the oligodendrocyte lineage. Cell 70:31–46

Baserga R (1985) The biology of cell reproduction. Harvard University Press, Cambridge

Bermingham-McDonogh O, Rubel EW (2003) Hair cell regeneration: winging our way towards a sound future. Curr Opin Neurobiol 13:119–126

Bhave SA, Stone JS, Rubel EW, Coltrera MD (1995) Cell cycle progression in gentamicin-damaged avian cochleas. J Neurosci 15:4618–4628

Bursch W, Kleine L, Tenniswood M (1990) The biochemistry of cell death by apoptosis. Biochem Cell Biol 68:1071–1074

Chardin S, Romand R (1995) Regeneration and mammalian auditory hair cells. Science 267:707–711

Chen P, Segil N (1999) p27(Kip1) links cell proliferation to morphogenes in the developing organ of Corti. Development 126:1581–1590

Chen P, Johnson JE, Zoghbi HY, Segil N (2002) The role of Math1 in inner ear development: uncoupling the establishment of the sensory primordium from hair cell fate determination. Development 129:2495–2505

Corwin T, Cotanche DA (1988) Regeneration of sensory hair cells after acoustic trauma. Science 240:1772–1774

Endo T, Nakagawa T, Lee JE, Dong Y, Kim TS, Iguchi F, Taniguchi Z, Naito Y, Ito J (2002) Alteration in expression of p27 in auditory epithelia and neurons of mice during degeneration. Neurosci Lett 334:173–176

Ferrari S, Battini R, Kaczmarek L, Rittling S, Calabretta B, Riel JK de, Philiponis V, Wei JF, Baserga R (1986) Coding sequence and growth regulation of the human vimentin gene. Mol Cell Biol 6:3614–3620

Forge A, Li L, Corwin JT, Nevill G (1993) Ultrastructural evidence for hair cell regeneration in the mammalian inner ear. Science 259:1616–1619

Izumikawa M, Minoda R, Kawamoto K, Abrashkin KA, Swiderski DL, Dolan DF, Brough DE, Raphael Y (2005) Auditory hair cell replacement and hearing improvement by Atoh1 gene therapy in deaf mammals. Nat Med 11:271–276

Kawamoto K, Ishimoto S, Minoda R, Brough DE, Raphael Y (2003) Math1 gene transfer generates new cochlear hair cells in mature guinea pigs in vivo. J Neurosci 23:4395–4400

Kil J, Gu R, Zhao YD, Hasson T, Lowenheim H, Fero M (2000) Inhibition of p27Kip1 induces hair cell regeneration in the organ of Corti. Assoc Res Otolaryngol Abstr 23:5510

Kuntz AL, Oesterle EC (1998) Transforming growth factor alpha with insulin stimulates cell proliferation in vivo in adult rat vestibular sensory epithelium. J Comp Neurol 399:413–423

Lang H, Fekete DM (2001) Lineage analysis in the chicken inner ear shows differences in clonal dispersion for epithelial, neuronal, and mesenchymal cells. Dev Biol 234:120–137

Lefebvre PP, Malgrange B, Staecker H, Moonen G, Van de Water TR (1993) Retinoic acid stimulates regeneration of mammalian auditory hair cells. Science 260:692–695

Li L, Forge A (1997) Morphological evidence for supporting cell to hair cell conversion in the mammalian utricular macula. Int J Dev Neurosci 15:433–446

Malek NP, Sundberg H, McGrew S, Nakayama K, Kyriakides TR, Roberts JM (2001) A mouse knock-in model exposes sequential proteolytic pathways that regulate p27Kip1 in G1 and S phase. Nature 413:323–327

Mantela J, Jiang Z, Ylikoski J, Fritzsch B, Zacksenhaus E, Pirvola U (2005) The retinoblastoma gene pathway regulates the postmitotic state of hair cells of the mouse inner ear. Development 132:2377–2388

Matei V, Pauley S, Kaing S, Rowitch D, Beisel KW, Morris K, Feng F, Jones K, Lee J, Fritzsch B (2005) Smaller inner ear sensory epithelia in Neurog1 null mice are related to earlier hair cell cycle exit. Dev Dyn 234:633–650

Oesterle EC, Sarthy PV, Rubel EW (1990) Intermediate filaments in the inner ear of normal and experimentally damaged guinea pigs. Hear Res 47:1–16

Raphael Y (2002) Cochlear pathology, sensory cell death and regeneration. Br Med Bull 63:25–38

Raphael Y, Altschuler RA (1991) Scar formation after drug-induced cochlear insult. Hear Res 51:173–183

Roberson DW, Rubel EW (1994) Cell division in the gerbil cochlea after acoustic trauma. Am J Otol 15:28–34

Rubel EW, Dew LA, Roberson W (1995) Mammalian vestibular hair cell regeneration. Science 267:701–707

Ruben RJ (1967) Development of the inner ear of the mouse: a radioautographic study of terminal mitoses. Acta Otolaryngol Suppl 220:1–44

Ryals BM, Rubel EW (1988) Hair cell regeneration after acoustic trauma in adult *Coturnix* quail. Science 240:1774–1776

Slepecky NB (1996) Structure of the mammalian cochlea. In: Dallos P, Popper AN, Fay RR (eds) The cochlea. Springer, Berlin Heiderberg New York, pp 46–129

Stone JS, Cotanche DA (1994) Identification of the timing of S phase and the patterns of cell proliferation during hair cell regeneration in the chick cochlea. J Comp Neurol 341:50–67

Stone JS, Rubel EW (2000) Temporal, spatial, and morphologic features of hair cell regeneration in the avian basilar papilla. J Comp Neurol 417:1–16

Stone JS, Choi YS, Woolley SM, Yamashita H, Rubel EW (1999) Progenitor cell cycling during hair cell regeneration in the vestibular and auditory epithelia of the chick. J Neurocytol 28:863–876

Thomaidou D, Mione MC, Cavanagh JFR, Parnavelas JG (1997) Apoptosis and its relation to the cell cycle in the developing cerebral cortex. J Neurosci 17:1075–1085

Voyvodic JT, Burne JF, Raff MC (1995) Identification of normal cell death in the rat retina: applications for normal composition in cell lineage analysis. Eur J Neurosci 7:2469–2478

West RA, Brummett RE, Himes DL (1973) Interaction of kanamycin and ethacrynic acid. Severe cochlear damage in guinea pigs. Arch Otolaryngol 98:32–37

Yaginuma H, Tomita M, Takashita N, McKay SE, Cardwell C, Yin Q-W, Oppenheim RW (1996) A novel type of programmed neuronal death in the cervical spinal cord of the chick embryo. J Neurosci 16:3685–3703

Yamasoba T, Schacht J, Shoji F, Miller JM (1999) Attenuation of cochlear damage from noise trauma by an iron chelator, a free radical scavenger and glial cell line-derived neurotrophic factor in vivo. Brain Res 815:317–325

Yamasoba T, Kondo K, Miyajima C, Suzuki M (2003) Changes in cell proliferation in rat and guinea pig cochlea after aminoglycoside-induced damage. Neurosci Lett 347:171–174

MIDAS/GPP34, a nuclear gene product, regulates total mitochondrial mass in response to mitochondrial dysfunction

Naomi Nakashima-Kamimura[1], Sadamitsu Asoh[1], Yoshitomo Ishibashi[1], Yuri Mukai[1,*], Yujiro Shidara[1,2], Hideaki Oda[2], Kae Munakata[3], Yu-ichi Goto[3] and Shigeo Ohta[1,‡]

[1]Department of Biochemistry and Cell Biology, Institute of Development and Aging Sciences, Graduate School of Medicine, Nippon Medical School, 1-396 Kosugi-cho, Kawasaki, Kanagawa, 211-8533, Japan
[2]Department of Pathology, Tokyo Women's Medical University, School of Medicine, Shinjuku-ku, Tokyo, 162-8666, Japan
[3]Department of Mental Retardation and Birth Defect Research, National Institute of Neuroscience, NCNP, Kodaira, Tokyo, 187-8502, Japan
*Present address: Computational Biology Research Center (CBRC), National Institute of Advanced Industrial Science and Technology (AIST), Koutou-ku, Tokyo, 135-0064, Japan
‡Author for correspondence (e-mail:ohta@nms.ac.jp)

Accepted 15 August 2005
Journal of Cell Science 118, 000-000 Published by The Company of Biologists 2005
doi:10.1242/jcs.02645

Summary

To investigate the regulatory system in mitochondrial biogenesis involving crosstalk between the mitochondria and nucleus, we found a factor named MIDAS (mitochondrial DNA absence sensitive factor) whose expression was enhanced by the absence of mitochondrial DNA (mtDNA). In patients with mitochondrial diseases, MIDAS expression was increased only in dysfunctional muscle fibers. A majority of MIDAS localized to mitochondria with a small fraction in the Golgi apparatus in HeLa cells. To investigate the function of MIDAS, we stably transfected HeLa cells with an expression vector carrying *MIDAS* cDNA or siRNA. Cells expressing the MIDAS protein and the siRNA constitutively showed an increase and decrease in the total mass of mitochondria, respectively, accompanying the regulation of a mitochondria-specific phospholipid, cardiolipin. In contrast, amounts of the mitochondrial DNA, RNA and proteins did not depend upon MIDAS. Thus, MIDAS is involved in the regulation of mitochondrial lipids, leading to increases of total mitochondrial mass in response to mitochondrial dysfunction.

Supplementary material available online at
http://jcs.biologists.org/cgi/content/full/118/22/5357/DC1

Key words: Mitochondria, Mitochondrial mass, Cardiolipin, Mitochondrial DNA, Mitochondrial disease, Golgi apparatus

Introduction

The mitochondrion is the center of energy metabolism in eukaryotes and has recently been recognized as a multifunctional organelle (Ohta, 2003). It is involved in the regulation of apoptosis as a reservoir of signals, regulators and executioners (Kroemer and Reed, 2000; Green and Kroemer, 2004). In addition, it functions as a source of reactive oxygen species, which are believed to cause many lifestyle-related diseases, neurodegenerative diseases, cancer and aging (Kowaltowski and Vercesi, 1999; Cortopassi and Wong, 1999; Melov, 2000). Thus, mitochondria are essential in many aspects of medicine as well as cell biology.

Depending on cell type, energy demands and physiological conditions, mitochondria vary in number, mass and morphology (Attardi and Schatz, 1988; Yaffe, 1999; Collins et al., 2002; Nisoli et al., 2003). The proliferation of cells usually accompanies an increase in mitochondria. However, an increase in number of mitochondria is not distinctly coordinated with the cell cycle. For example, muscle mitochondria increase in response to exercise, independently of cell division (Brunk, 1981; Moyes et al., 1997). Exposure to a low-temperature environment or cultivation in glucose-deprived medium induces a marked increase in mitochondrial mass (Klaus et al., 1991; Weber et al., 2002). In addition, mitochondria increase in response to external stimuli with a wide range of substances including benzodiazepine, phorbol esters, calcium fluxes (Bereiter-Hahn and Voth, 1994; Vorobjev and Zorov, 1983; Muller-Hocker et al., 1986; Kawahara et al., 1991), thyroid hormones (Goglia et al., 1999) and nitric oxide (NO) (Nisoli et al., 2004). Mitochondrial numbers also increase in response to internal stimuli, such as the mitochondrial dysfunction caused by pathogenic mtDNA mutations (Schon, 2000; Wallace, 1999; Moraes et al., 1992). An increase in mitochondrial mass was observed in mitochondrial transcription factor A (*Tfam*) knockout mice, which have depleted mtDNA (Hansson et al., 2004).

As nuclear genes encode most mitochondrial proteins, including the enzymes and cofactors required for the transcription and replication of mtDNA, mitochondrial biogenesis depends on a distinct crosstalk between two physically separated genetic systems (Garesse and Vallejo, 2001). Recently, the pathway that links external physiological stimuli to the regulation of mitochondrial biogenesis and function has been studied. Several transcription/replication factors directly regulate mitochondrial genes and the

coordination of these factors into a programmed response to the environment was reported (Scarpulla, 2002).

However, the nature of mitochondrial biogenesis in response to internal stimuli is poorly understood. Mitochondrial stress results in enhanced expression of sarcoplasmic reticular ryanodine receptor-1 and some Ca^{2+}-responsive transcription factors (Biswas et al., 1999). Several tumor-specific markers are overexpressed in cells subjected to mitochondrial genetic as well as metabolic stress (Amuthan et al., 2001). Moreover, we have reported that expression of the apoptosis-mediator Fas is enhanced by dysfunctional mitochondria (Asoh et al., 1996). However, no one has reported on the mammalian factors, in response to a signal from mitochondria to the nucleus, which are involved in the stimulation of mitochondrial growth. Notably, the molecular mechanism regulating the biogenesis of mitochondrial lipids is poorly understood.

In this study, we identified factors whose expression was enhanced by depletion of mtDNA. One of them was found to increase total mitochondrial mass without a pathogenic swelling, when overexpressed. Thus, the factor is involved in the accumulation of mitochondria in response to mitochondrial dysfunction.

Materials and Methods

Cells and culture

EB8 and Ft2-11 were described previously (Hayashi et al., 1991; Hayashi et al., 1994). EB8 is a clone, derived from HeLa cells, completely lacking mtDNA, whereas Ft2-11 was constructed by transferring wild-type mtDNA into EB8 so that Ft-2-11 has the same nucleus as EB8. Stable transfectants expressing MIDAS constitutively were constructed from HeLa cells by transfection with *MIDAS* cDNA under the control of the CMV promoter or its empty vector (pCMV-SPORT; Life Technologies).

Stable transfectants expressing siRNA of *MIDAS* were constructed from HeLa cells by transfection with the pSilencer vector (Ambion) with inserts targeting *MIDAS* (5′-AAGCTTTTCCAAAAAAGTGG-AATGTCTGAAGGCCATCTCTTGAATGGCCTTCAGACATTCC-ACGGGATCC-3′) or a random sequence.

HeLa cells and stable transfectants were cultured in DMEM/F-12 (1:1) (Gibco-BRL) supplemented with 10% FBS and 1% penicillin/streptomycin (Gibco-BRL).

Construction of Myc-tagged MIDAS

To insert the Myc tag at the N-terminus of MIDAS, an *Eco*RI site was generated at the 5′ end of the *MIDAS* coding sequence by PCR and was cloned into the pCMV-SPORT vector. An oligonucleotide encoding MEQKLISEEDLNS (Myc tag sequence underlined) was inserted at the newly generated *Eco*RI site of *MIDAS*. To construct the Myc tag at the C-terminus of MIDAS, a *Bam*HI site was generated at the 3′ end of the coding sequence and an oligonucleotide encoding DPEQKLISEEDL was inserted.

Differential display

Poly(A)$^+$ RNA was purified from Ft2-11 and EB8 and reverse transcribed. Resultant cDNAs were amplified using arbitrary primer sets, followed by 5% PAGE. The gel was stained with Vistra Green (Amersham Biosciences) and visualized with a Fluoro Imager (Molecular Dynamics) (Liang and Pardee, 1992).

Antibodies

Anti-MIDAS polyclonal rabbit antiserum was raised against His-tagged MIDAS expressed in *Escherichia coli*. Anti-MIDAS antibody was affinity purified by binding to the MIDAS protein isolated by SDS-PAGE, followed by transfer onto a PVDF membrane. Anti-Tom20 and anti-Tom40 were gifts from K. Mihara, Kyushu University, Japan. Other antibodies were purchased as follows: anti-actin (clone AC-40) and anti-β-tubulin from Sigma; anti-p230 antibody and anti-Syntaxin6 from BD Biosciences; anti-Hsc70 antibody from Santa Cruz; anti-Hsp60 from MBL; anti-cytochrome c antibody and anti-Cox4 from Clontech; and anti-SDH70, anti-SDH30, anti-COX I and anti-COX II antibodies from Molecular Probes.

Immunohistochemical staining of muscle sections

Biopsy samples were obtained from the biceps brachii muscle with informed consent and then frozen in isopentane and liquid nitrogen. Frozen sections 6 μm thick were stained histochemically and immunologically. Activities of SDH and COX were visualized as described previously (Hasegawa et al., 1991; Dubowitz, 1985). The expression of MIDAS was detected with anti-MIDAS antibody. The polyclonal antibody against MIDAS was diluted 500-fold with 10% BSA in PBS and incubated with sections for 5 hours at 37°C and then MIDAS was detected with DAB using an indirect streptavidin-biotin immunohistochemical method, according to the manufacturer's protocol (Histofine, Nichirei, Co. Ltd., Tokyo, Japan). The MIDAS protein expressed was semi-quantified by the density of staining.

Immunocytostaining of cultured cells

Cultured cells were fixed with 4% paraformaldehyde in PBS for 20 minutes at room temperature. After a wash with PBS, they were treated with 5% acetic acid in ethanol for 10 minutes at –20°C to permeabilize membranes, then incubated in a blocking buffer (3% BSA and 3% goat serum in PBS) and overnight at 4°C in the blocking buffer containing primary antibody. After another wash with PBS, the cells were incubated in the blocking buffer containing labeled secondary antibody and visualized with a confocal laser-scanning microscope (Fluoview FV300, Olympus, Tokyo, Japan). As an alternative, we used another method described (Bell et al., 2001). In brief, cells were fixed for 10 minutes with 4% paraformaldehyde and 4% sucrose without treatment for permeabilization and incubated with primary antibody, followed by secondary antibody.

Subfractionation of HeLa cells

Cells were homogenized as described (Trounce et al., 1996). The homogenate was applied to a 7-35% (w/v) Nycodenz preformed continuous density gradient and centrifuged in a swinging-bucket rotor at 77,000 g_{AV} for 4 hours. The fractions were collected from the top of the gradient. The MIDAS protein was semi-quantified by the density of total bands in western blots. The sub-organellar fractionation of mitochondria (fraction number 15) was performed as described (Kanamori et al., 2003).

Electron microscopy

Cells were cultured on plastic dishes and fixed with 2% glutaraldehyde in PBS. Ultra-thin sections were stained with uranyl acetate and lead nitrate and examined with an H-7000 electron microscope (Hitachi, Tokyo, Japan).

Flow cytometry

Living transfectants were stained with 20 nM MitoTracker Red CMXRos (Molecular Probes) or 100 nM MitoTracker Green (Molecular Probes) for 30 minutes at 37°C, treated with trypsin and subjected to a flow cytometric analysis with an Epics Elite ESP (Coulter).

Three-dimensional imaging

Living cells were stained with 20 nM MitoTracker Red and 500 nM SYTO 16 (Molecular Probes) for 30 minutes at 37°C. The cells were scanned using 0.4 μm sections with the confocal laser-scanning microscope. Three-dimensional (3D) views were reconstructed with Fluoview software (Olympus) and volumes of the nucleus and mitochondria were calculated by summing fluorescent areas from each section using the NIH Image program (developed at the US National Institutes of Health and available on http://rsb.info.nih.gov./nih-image).

Separation of phospholipids

Total lipids were extracted from transfectants using methanol/chloroform as described (Folch et al., 1957). For the separation and detection of phospholipids, total lipids were injected into a HPLC system (model 616; Waters) fitted with a Wakosil 5Sil column (Wako, Tokyo, Japan). The mobile phase was a mixture of n-hexan, isopropanol, ethanol, acetic acid and 25 mM potassium phosphate buffer (pH 7.0) (146:282.5:50:0.3:31; v/v/v/v/v). The flow rate was 1 ml/minute. The elution of phospholipids was monitored at 205 nm with the UV detector (SPD-10A; Shimadzu). Retention times and quantities of phospholipids were determined using a phospholipid kit (Doosan Serdary Research Laboratory) as a standard.

Results

Cloning of genes that respond to a depletion of mtDNA

To identify nuclear genes that respond to a depletion of mtDNA, we screened for mRNA whose expression increased in cells lacking mtDNA using the differential mRNA display technique (Liang and Pardee, 1992) (Fig. 1A) by comparing mRNA populations in a HeLa derivative lacking mtDNA (EB8) (Hayashi et al., 1991) and control cybrid cells (Ft2-11) (Hayashi et al., 1994). Bands 1 and 2, which were stronger in EB8 than in Ft2-11 (Fig. 1A), were found to correspond to the apurinic/apyrimidinic endonuclease I (APE1/HAP1) (Demple et al., 1991) and DNA ligase III genes (Wei et al., 1995), respectively. The products of these genes are localized in mitochondria and involved in mtDNA repair (Kang and Hamasaki, 2002).

DNA sequencing distinguished the gene corresponding to the third band in Fig. 1A from the genes which have been so far identified to be involved in mitochondrial biogenesis, gene expression and metabolism. The full-length cDNA was isolated from a human brain cDNA library (Gibco-BRL) to confirm the increase in its mRNA (Fig. 1B,C) and its product (Fig. 1D,E) by northern and western blotting, respectively. We named this gene *MIDAS* (mitochondrial DNA absence sensitive factor), because the gene product was expressed in response to mtDNA depletion. Interestingly, the nucleotide sequence was identical to *GPP34* (GenBank accession no. AJ296152) whose product has been identified as a Golgi protein of unknown function(s) (Bell et al., 2001). In addition, MIDAS/GPP34 contains an isoform named GPP34R (GenBank accession no. AJ296153), which is highly homologous with MIDAS/GPP34 (supplementary material Fig. S1). In fact, GPP34R was expressed in cells with the HeLa nucleus as detected by northern blotting (supplementary material Fig. S2A). Interestingly, GPP34R was also expressed more abundantly in EB8 than in Ft2-11 (supplementary material Fig. S2A). The relative amount of GPP34R mRNA was semi-quantified by the TaqMan probe method and found to be less than 2% of that in

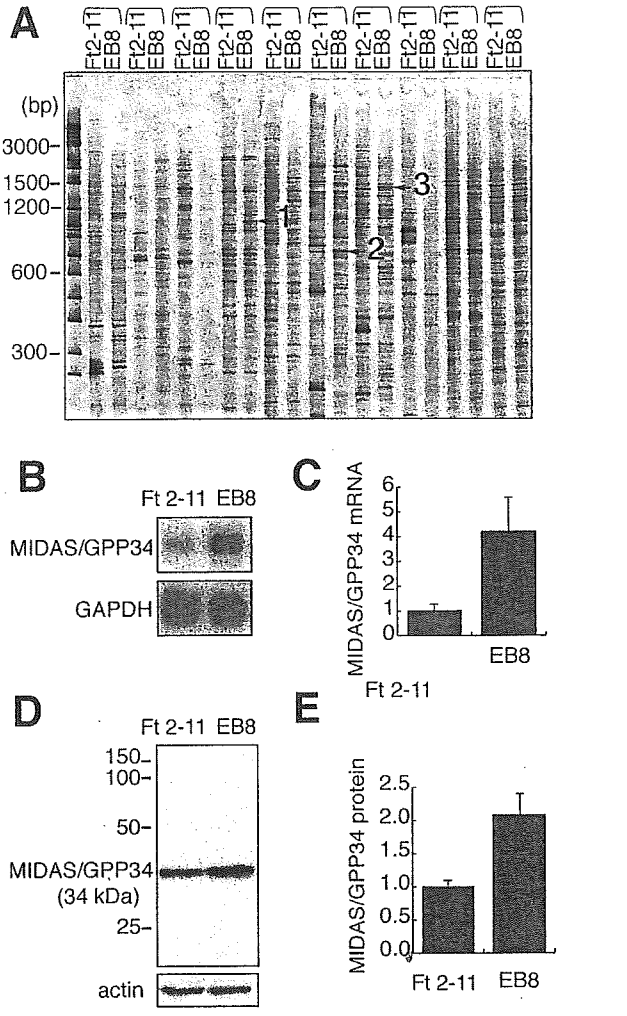

Fig. 1. Enhanced expression of MIDAS/GPP34 in EB8 (mtDNA-free HeLa cells). (A) Comparison of mRNA obtained from Ft2-11 with that from EB8 by differential display. EB8 lacks mtDNA whereas Ft2-11 is derived from EB8 but has wild-type mitochondria. Ten sets of arbitrarily primed PCR products were subjected to 5% PAGE. Three bands indicated by arrows were cloned and sequenced. Bands 1, 2 and 3 corresponded to apurinic/apyrimidinic endonuclease I, DNA ligase III and MIDAS/GPP34, respectively. (B) Northern blots of total RNA extracted from Ft2-11 and EB8 were hybridized with *GPP34*- and *GAPDH* (glyceraldehyde-3-phosphate dehydrogenase)-specific probes. (C) *GPP34* mRNA levels normalized to *GAPDH* levels based on the mean values±s.d. for three sets of northern blotting experiments (vertical bars). (D) Western blotting of Ft2-11 and EB8. Whole-cell lysates were separated by 12% SDS-PAGE and transferred onto a PVDF membrane. MIDAS/GPP34 was immunostained with anti-MIDAS antibody. (E) The MIDAS/GPP34 protein normalized against actin. Mean values of three sets of experiments are shown with s.d. (vertical bars).

MIDAS/GPP34 (supplementary material Fig. S2B). Therefore, we focused on the function of MIDAS/GPP34.

Specific expression of MIDAS/GPP34 in muscle fibers with abnormal mitochondria

Mitochondria accumulate in response to their own dysfunction

in mitochondrial diseases (Schon, 2000; Wallace, 1999). We examined the expression of MIDAS/GPP34 in muscle fibers of patients with mitochondrial diseases. Large deletions and a point mutation in the $tRNA^{Leu(UUR)}$ gene of mtDNA are responsible for the subgroups of mitochondrial diseases, CPEO (chronic progressive external ophthalmopelia) (Holt et al., 1988; Shoubridge et al., 1990) and MELAS (mitochondrial myopathy, encephalopathy, lactic acidosis and stroke-like episodes) (Goto et al., 1990; Kobayashi et al., 1990; Kobayashi et al., 1991), respectively. Accumulations of abnormal mitochondria are detected as ragged-red fibers and high succinate dehydrogenase (SDH) fibers, with mutant mtDNA dominating in a mosaic manner (Engel and Cunningham, 1963; Hasegawa et al., 1991; Lightowlers et al., 1997).

Muscle sections from a normal subject and patients with CPEO or MELAS were stained for activity of SDH and cytochrome c oxidase (COX) and with anti-MIDAS antibody. No MIDAS-positive fibers were detected in normal muscle, whereas MIDAS-positive fibers were detected in the muscle sections of affected patients (Fig. 2). The amount of MIDAS in the positive muscles increased approximately twofold compared to those in the negative muscles. It is noted that MIDAS was more abundant specifically in fibers with an SDH^{++}/COX^{-} phenotype (Fig. 2, asterisks). Thus, MIDAS is expressed in response to mitochondrial dysfunction in muscle with mitochondrial diseases.

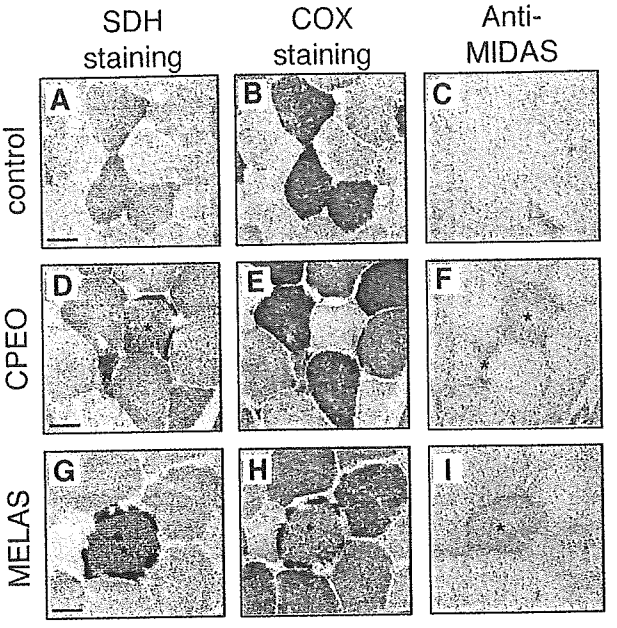

Fig. 2. Expression of MIDAS/GPP34 in SDH^{++}/COX^{-} muscle cells of patients with mitochondrial diseases. Biopsy samples were obtained from the biceps brachii muscle. Activities of SDH and COX were visualized histochemically and the expression of MIDAS/GPP34 was detected with anti-MIDAS antibody. (A-C) Control muscle without mitochondrial disorder. (D-F) Muscle from a patient with CPEO who has a common deletion in mtDNA. (G-I) Muscle from a patient with MELAS who has a point mutation at nucleotide number 3243 in the $tRNA^{Leu(UUR)}$ gene. Asterisks indicate SDH^{++}/COX^{-} cells of patients with increased MIDAS/GPP34 expression. Bars, 50 μm.

Subcellular distribution of MIDAS/GPP34

GPP34 has been isolated as a Golgi peripheral membrane protein in a Golgi proteomics study (Bell et al., 2001). To verify the distribution of MIDAS in mitochondria, we immunostained HeLa cells with an affinity-purified polyclonal antibody against the MIDAS protein. Immunostaining of HeLa cells revealed that MIDAS mainly colocalized with MitoTracker Red (Fig. 3A). The mitochondrial localization was confirmed with another mitochondrial marker, Hsp60 (data not shown). With careful observation, we found MIDAS in an additional region, the perinuclear area, where MitoTracker Red was absent (Fig. 3A, merge; indicated by white arrowhead). This region corresponds to the Golgi apparatus, as judged by immunostaining with anti-p230 (the *trans*-Golgi membrane protein) (Erlich et al., 1996) antibody (Fig. 3B). These results suggest that a majority of MIDAS/GPP34 localizes to mitochondria, but some is distributed in the Golgi apparatus.

This finding disagrees with the previous study on GPP34 showing that GPP34 is located in the Golgi apparatus, but not in mitochondria (Bell et al., 2001). This discrepancy could be due to a different fixation method prior to staining. In general, for immunostaining of cultured cells, the permeabilization of intramembranes with an organic solvent or detergent is essential for antibodies to penetrate the membranes of organelles (Zeller, 1998). In fact, under the same conditions as the published experiment (no permeabilization pretreatment), MIDAS did not show colocalization with mitochondria (Fig. 3D), being detected only in the Golgi apparatus (Fig. 3E). Moreover, several marker proteins were immunostained to confirm that the permeabilization pretreatment with acetate in cold ethanol is essential for detecting the mitochondrial proteins located internally. Without permeabilization pretreatment, cytosolic (Hsc70), mitochondrial outer membrane (Tom20) and *trans*-Golgi (p230) proteins were stained with each antibody (Fig. 3F), whereas the mitochondrial intermembrane space protein (cytochrome c) could not be detected (Fig. 3F). Alternatively, cytochrome c required an acetate/ethanol pretreatment for permeabilization as described in Materials and Methods to be detected (Fig. 3C). Moreover, a mitochondrial matrix protein (Hsp60) and an inner membrane protein (SDH70) were clearly stained only with the acetate/ethanol pretreatment (supplementary material Fig. S3). Therefore, the mitochondrial MIDAS/GPP34 protein is located inside mitochondria or embedded in the outer membrane. In addition, immunostaining with anti-KDEL, the signal peptide targeting the endoplasmic reticulum (ER) (Munro and Pelham, 1987), showed no localization of MIDAS/GPP34 to the ER (data not shown).

To further investigate the subcellular distribution of MIDAS, Myc-tagged constructs were generated. A gene corresponding to a Myc peptide was fused to the gene of the N-terminus (Myc-MIDAS) or C-terminus (MIDAS-Myc) of MIDAS. Fusion constructs were transfected into HeLa cells and the cells were allowed to express the protein for 16 hours. The transfected cells were immunostained with anti-Myc antibody. Myc-MIDAS was localized to the perinuclear area and colocalized with the p230 *trans*-Golgi (Fig. 3G). On the other hand, MIDAS-Myc was distributed in both mitochondria and Golgi as stained with anti-MIDAS antibody (Fig. 3H). This

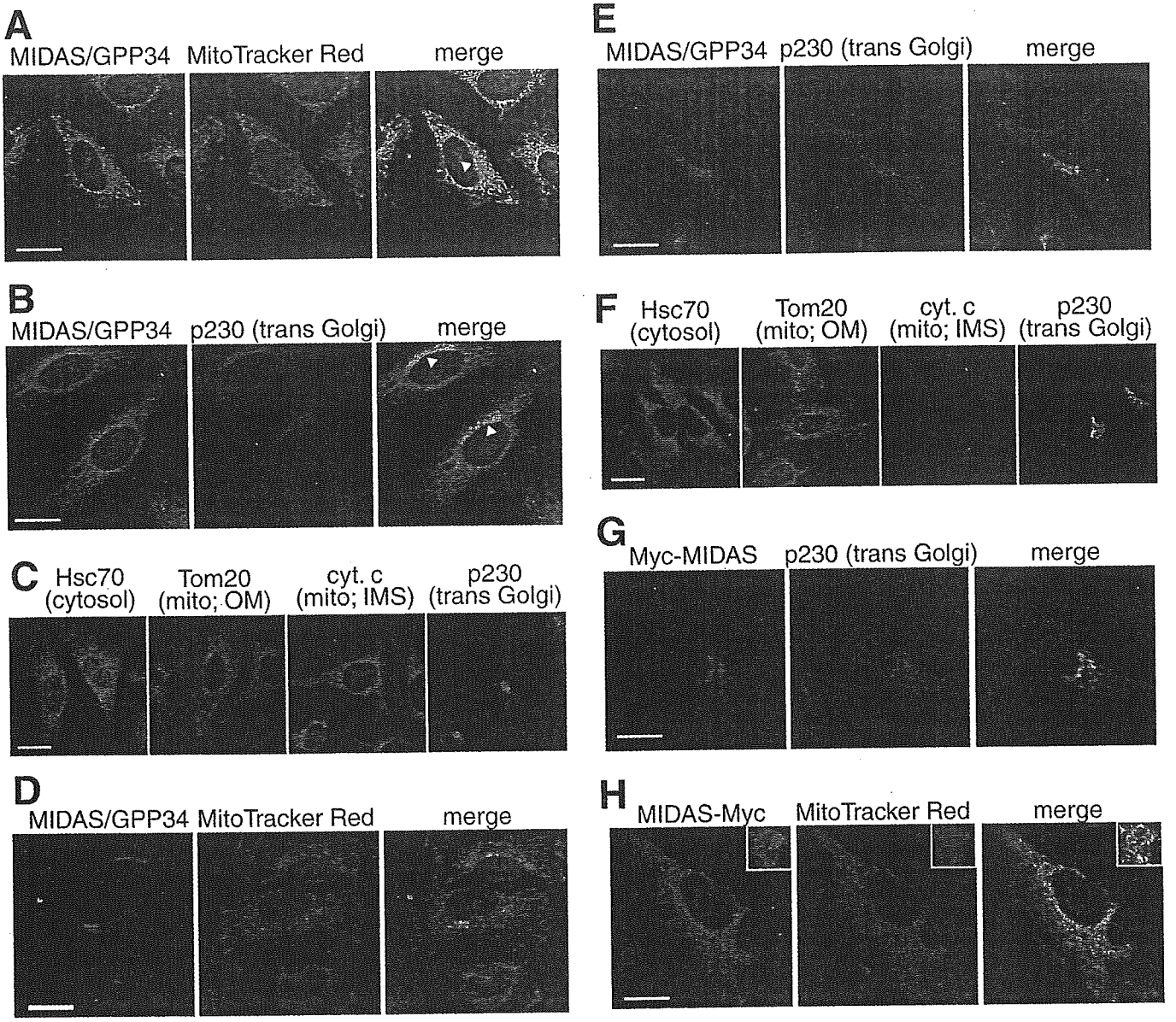

Fig. 3. Localization of MIDAS/GPP34 in mitochondria and the Golgi apparatus. (A-C) HeLa cells in culture were fixed, permeabilized with 5% acetic acid in ethanol and then immunostained with various antibodies. (A) MitoTracker Red (100 nM) was added as a mitochondrial indicator prior to fixation. MIDAS/GPP34 was detected with anti-MIDAS antibody. Arrowhead indicates where MIDAS/GPP34 is more abundant than mitochondria in a perinuclear area. (B) MIDAS/GPP34 and p230 (*trans*-Golgi) were double-stained immunochemically using different secondary antibodies. Arrowheads indicate where the perinuclear area was co-stained with both antibodies. (C) Hsc70 (cytosol), Tom20 (outer membrane of mitochondria), cytochrome c (cyt. c) (intermembrane space of mitochondria) and p230 (*trans*-Golgi) were detected with their respective antibodies. (D-F) HeLa cells in culture were fixed with 4% paraformaldehyde and 4% sucrose without treatment for permeabilization and immunostained with the same procedure as in (A-C). (G,H) Localization of Myc-tagged MIDAS. A Myc tag was fused to the N-terminus (G) or C-terminus (H) of MIDAS. Fusion constructs were transfected into HeLa cells and cells were allowed to express protein for 16 hours. Cells were stained with anti-Myc, anti-p230 antibodies or MitoTracker Red with the same procedure as in (A-C). Bars, 20 μm.

finding suggests that MIDAS potentially localizes to both mitochondria and the Golgi apparatus.

To demonstrate the subcellular distribution of MIDAS, organelles were sub-fractionated with a Nycodenz gradient. HeLa cells were homogenized, the homogenate was fractionated with a 7-35% density gradient and the distribution of MIDAS was examined by western blotting (Fig. 4A). The majority of MIDAS was detected in the mitochondrial fractions (with Tom20 and Hsp60) and small portions were fractionated with the Golgi (with a Golgi marker, Syntaxin6) and cytosol. Relative amounts of MIDAS distributed in the fractions for mitochondria (fractions 13-17), Golgi (fractions 6-12) and cytosol (fractions 1-5) were 0.75, 0.19 and 0.06, respectively, as judged by the densities of total bands.

To determine the sub-mitochondrial distribution of MIDAS, the mitochondria purified from HeLa cells were treated with

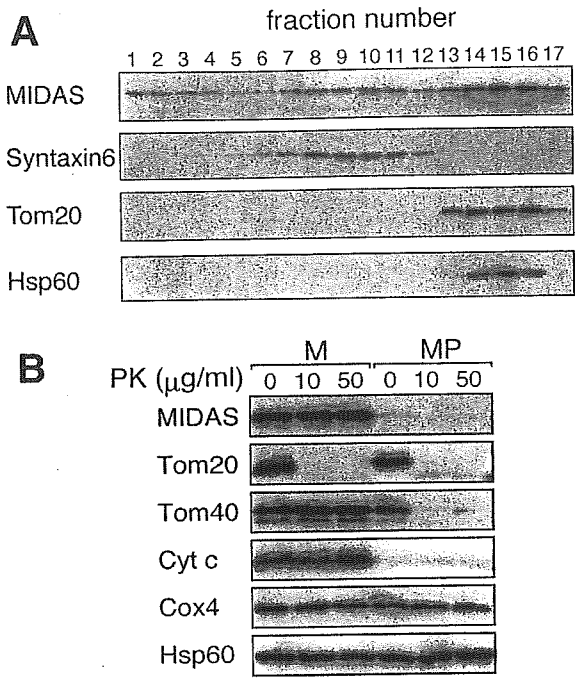

Fig. 4. Localization of MIDAS/GPP34 in the mitochondrial intermembrane space. (A) Fractionation of organelles of HeLa cells in 7-35% (w/v) preformed density gradients. The distribution of MIDAS was detected by western blotting. Syntaxin6 was used for a Golgi marker. Tom20 and Hsp60 were used for mitochondrial markers. (B) Mitoplasts were obtained from the mitochondrial fraction (fraction 15 in A) by osmotic disruption of the outer membrane. The mitochondria (M; lanes 1-3) and the mitoplasts (MP; lanes 4-6) were treated with proteinase K (PK; 10 μg/ml or 50 μg/ml). Mitochondrial sub-fractions were monitored by western blotting with antibodies directed against Tom20 (an outer membrane protein; most of which is exposed outside mitochondria), Tom40 (an outer membrane protein), cytochrome c (cyt c) (an intermembrane space protein), Cox4 (an inner membrane protein) and Hsp60 (a matrix space protein).

proteinase K. Both Tom40 and Tom20 are embedded in the outer membrane, whereas Tom20 is exposed to the outside of mitochondria (Pfanner and Geissler, 2001). Tom20 was easily digested with 10 μg/ml proteinase K, whereas Tom40 and MIDAS were resistant (Fig. 4B, M). On the other hand, when mitochondria were converted to mitoplasts, MIDAS disappeared (Fig. 4B, MP) even without proteinase K, as cytochrome c disappeared. From these results, it was concluded that the majority of MIDAS protein is located in the intermembrane space of mitochondria, with a small fraction present in the Golgi apparatus.

Mitochondrial accumulation without swelling by MIDAS

To determine the function of MIDAS in mitochondria, HeLa cells were transfected with *MIDAS* cDNA under the control of the CMV promoter. We could isolate transfectants constitutively expressing MIDAS at low levels (1.5- to 2-fold increase) (Fig. 5A, upper left panel, CMV-MIDAS3 and CMV-MIDAS9). Cells transiently transfected with a higher level of MIDAS could undergo cell division once or twice but did not survive for a week (data not shown), suggesting that overproduction of MIDAS prevents cell growth. To downregulate MIDAS, we then constructed HeLa transfectants expressing siRNA (small interfering RNA) of *MIDAS* to inhibit the endogenous MIDAS expression (Fig. 5A, upper right panel).

These transfectants were stained with MitoTracker Red to visualize mitochondria, in a short period to monitor the membrane potential of mitochondria. Even low levels of additional MIDAS expression caused a change in the distribution of mitochondria. The mitochondria in a *MIDAS* transfectant CMV-MIDAS3 were concentrated around the nucleus (Fig. 5B, second panel), whereas those in the control transfectants remained dispersed (Fig. 5B, first panel).

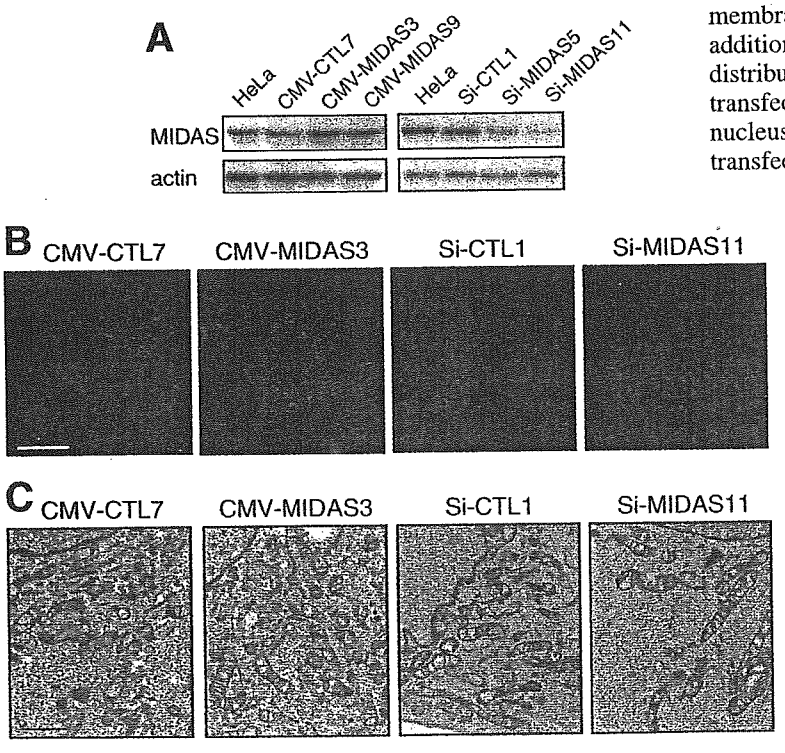

Fig. 5. The increased or decreased mass of intact mitochondria related to MIDAS concentration. (A) CMV-CTL7 and Si-CTL1 are stable control transfectants derived from HeLa cells. Although CMV-MIDAS3 and CMV-MIDAS9 are stable *MIDAS* transfectants under the control of the CMV promoter. Si-MIDAS5 and Si-MIDAS11 were transfectants expressing siRNA of *MIDAS* constitutively. Total cell lysate was extracted from each transfectant cell line and subjected to western blotting with anti-MIDAS and anti-actin antibodies. (B) Control (CMV-CTL7 and Si-CTL1), *MIDAS* transfectants (CMV-MIDAS3) and siRNA *MIDAS* transfectants (Si-MIDAS11) were stained with MitoTracker Red and visualized by confocal scanning laser microscopy. (C) Electron micrographs (×8000) of mitochondria in the transfectants. Bar, 20 μm (B); 1 μm (C).

Moreover, mitochondria in the MIDAS-expressing transfectants were stained more strongly than those in the control cells. Another transfectant clone CMV-MIDAS9 showed the same results (data not shown).

The mitochondria in a siRNA *MIDAS* transfectant, Si-MIDAS11, were dispersed similarly to those in the control transfectant (Si-CTL1) but were less intensely stained (Fig. 5B, third and fourth panels). Another siRNA *MIDAS* transfectant, clone Si-MIDAS5, showed the same results (data not shown).

Electron microscopy showed that mitochondria in the *MIDAS* transfectant were somewhat larger with no marked change in morphology and were neither pathologically swollen nor had lost the cristae structure (Fig. 5C, second panel). In addition, the *MIDAS* transfectants increased the number of mitochondria, whereas the siRNA-transfectants decreased the number of mitochondria (Fig. 5C, fourth panel). These photographs suggest that the number of mitochondria around the nucleus was increased by MIDAS.

Increase in total mitochondrial mass by MIDAS

To quantify the accumulation of mitochondria suggested above, cells were stained with two mitochondria-specific dyes, MitoTracker Red and MitoTracker Green and subjected to flow cytometric analysis (Fig. 6A-C). There was no significant difference in forward scatter among any of the cells examined (FS in Fig. 6C), indicating that MIDAS does not have any influence on cell size, regardless of the up- or downregulation of its expression. MitoTracker Green, but not MitoTracker Red, binds to mitochondria in a membrane-potential-independent manner and fluoresces only in the lipid environment of mitochondria. Fluorescent intensity in green (MitoTracker Green) was measured to estimate overall mitochondrial mass, whereas fluorescent intensity in red (MitoTracker Red) was measured to assess the content of energized mitochondria. The intensities in green and red significantly increased in MIDAS-expressing transfectants (CMV-MIDAS) (Fig. 6A,C). On the other hand, the green and red intensities decreased in the MIDAS downregulated transfectants (Si-MIDAS) (Fig. 6B,C). Quantitative analysis showed that the fluorescent intensities increased 1.5- to 2-fold in the MIDAS-expressing transfectants and decreased to 60-70% in the downregulated transfectants, compared to the control cells, respectively (Fig. 6C). The ratio of the intensity in red to the intensity in green was the same in all the cells examined, indicating that MIDAS does not exert any influence on the membrane potential. To confirm the increase in mitochondria, we stained transfectants with an additional fluorescent dye, TMRM (tetra-methyl-rhodamine methyl ester) specific to mitochondria and obtained a consistent result (supplementary material Fig. S4).

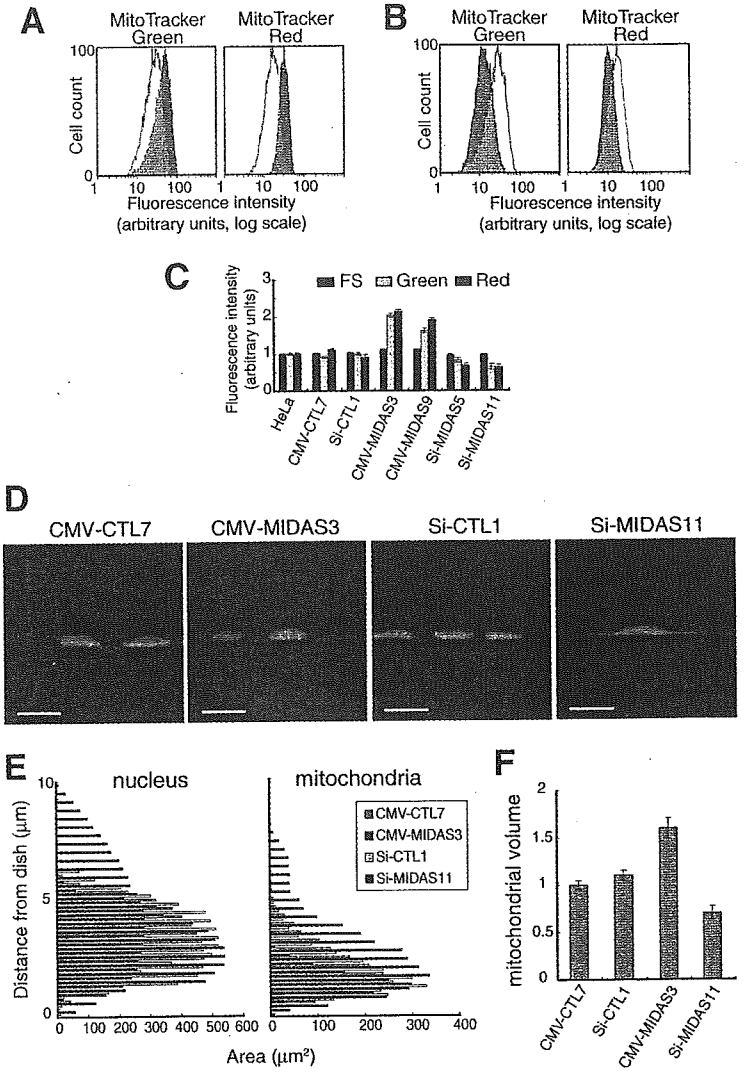

Fig. 6. Changes in mitochondrial mass with MIDAS. (A) Flow cytometric profiles of the fluorescence of dyes specific to mitochondria in CMV-CTL7 (white) and CMV-MIDAS3 (gray). Living transfectants were stained with MitoTracker Green (left) or MitoTracker Red (right) and analyzed with a flow cytometer. (B) Flow cytometric analysis performed with Si-CTL1 (white) and Si-MIDAS11 (gray) cells as described in A. (C) Fluorescence intensity (MitoTracker Green and MitoTracker Red) as well as forward scatter (FS) of HeLa cells and transfectants as quantified by flow cytometry. Values are the mean±s.d. (D) The mitochondria and nucleus in control transfectants (CMV-CTL7 and Si-CTL1), *MIDAS* transfectants (CMV-MIDAS3) and siRNA *MIDAS* transfectants (Si-MIDAS11) were stained with MitoTracker Red and SYTO 16 (green), respectively and scanned by confocal laser microscopy in each 0.4 μm section. Then the side view of a three-dimensional image was reconstructed with Fluoview software. (E) Areas of the nucleus and mitochondria were measured for each section. (F) The total mass of mitochondria in the transfectants was calculated based on the values in E and normalized to that of nucleus. Data represent the mean±s.d. of three sets of experiments. Bars, 20 μm.

The increase in the fluorescence of MitoTracker Green strongly suggests a substantial increase in total mitochondrial mass caused by MIDAS. Therefore, we estimated total mitochondrial volume by three-dimensional reconstitution of cells. Cells were stained with MitoTracker Red (red) for mitochondria and SYTO 16 (green) for the nucleus, respectively. The cells were scanned from bottom to top at intervals of 0.4 μm and each image was analyzed to measure the areas stained with MitoTraker Red and SYTO 16,

separately (Fig. 6E). Interestingly, the side view of the reconstituted three-dimensional image showed that mitochondria in the transfectants expressing MIDAS accumulated at the periphery of the nucleus (Fig. 6D, second panel), whereas in the downregulated transfectants, mitochondria appeared to be decreased in number (Fig. 6D, fourth panel). It is noted that there was no difference in nuclear volume between cells, although their three-dimensional shapes were different. On average, mitochondria occupied 22%, 35% and 15% of the total cytoplasm in controls, MIDAS-expressing transfectants and siRNA transfectants, respectively. The total volume of mitochondria was increased 1.6-fold by the MIDAS expression and decreased 0.75-fold by the downregulation of MIDAS, when normalized to that of the nucleus (Fig. 6F). Thus, the total mitochondrial mass varied more than 2.3-fold with the up- and downregulation of MIDAS. These results clearly indicate that MIDAS regulates total mitochondrial mass.

Regulation of cardiolipin by MIDAS

Flow cytometric analysis using MitoTracker Green showed that mitochondrial lipids varied in a MIDAS-dependent manner. Furthermore, the analysis using the fluorescent dye NAO (nonyl acridine orange), which detects cardiolipin, a mitochondria-specific phospholipid, revealed that the amount of cardiolipin varied according to amount of MIDAS (supplementary material Fig. S5). To obtain direct evidence for an increase in mitochondrial lipids caused by MIDAS, we measured levels of cardiolipin by HPLC. Total lipids were extracted from each transfectant and separated by HPLC as described in the Materials and Methods (Fig. 7A). The peak of cardiolipin (CL) was found to increase in MIDAS-expressing transfectants, compared with control transfectants. In clear contrast, the CL peak decreased in the MIDAS downregulated transfectants. The relative amount of each phospholipid was quantified based on the HPLC peak (Fig. 7B). The results showed that the amount of cardiolipin was increased 1.75-fold in the MIDAS-expressing transfectant and decreased 0.65-fold in the downregulated transfectant, when normalized to that of phosphatidylcholine. Thus, the amount of cardiolipin varied more than 2.6-fold with the up- and downregulation of MIDAS.

Mitochondrial DNA, RNA and proteins were not affected by MIDAS

To understand the mitochondrial increase induced by MIDAS, we examined other mitochondrial components, mitochondrial DNA, RNA and proteins (Fig. 7C). The amount of mtDNA was analyzed by Southern blotting and no significant change was observed. Northern blotting also revealed no change in the stationary amounts of COX II mRNA transcribed from mtDNA. Immunoblots revealed no increase in mitochondrion-

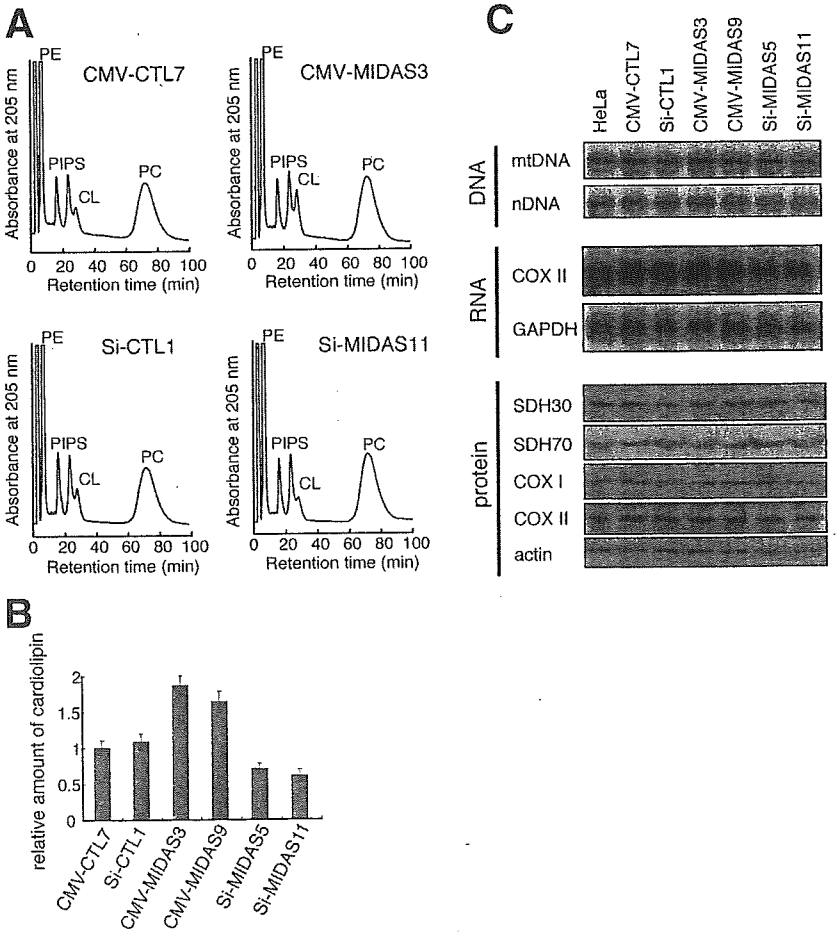

Fig. 7. Effects of MIDAS on amounts of cardiolipin (a mitochondria-specific lipid), mitochondrial DNA, RNA and proteins. (A) Total lipids were extracted from control transfectants (CMV-CTL7 and Si-CTL1), *MIDAS* transfectants (CMV-MIDAS3) and siRNA *MIDAS* transfectants (Si-MIDAS11) and fractionated by HPLC as described in the Materials and Methods. The elution of phospholipids was monitored at 205 nm. CL, cardiolipin; PC, phosphatidylcholine; PE, phosphatidylethanolamine; PI, phosphatidylinositol; PS, phosphatidylserine. (B) The amount of cardiolipin in the transfectants was quantified based on the values in A and normalized to that of phosphatidylcholine. Mean values for three sets of experiments are shown with the s.d. (C) The amount of DNA in HeLa cells and transfectants was analyzed by Southern blotting. To detect mtDNA we used the COX II region in mtDNA as a probe. The nDNA (nuclear DNA) was a loading control and the 18S ribosomal DNA region was used as a probe. The expression of mtDNA and nDNA was analyzed by northern blotting. Blots of total RNA extracted from HeLa and transfectants were hybridized with *COX II*- and *GAPDH* -specific probes. Proteins were analyzed by western blotting. SDH30 and SDH70 are the nucleus-encoded 30 kDa and 70 kDa subunit of SDH, respectively. COX I and COX II are the mitochondrial DNA-encoded subunits.

encoded proteins, COX I and COX II and nucleus-encoded mitochondrial proteins, the 30 kDa and 70 kDa subunits of SDH.

Discussion

In this study, we found three nuclear genes that respond to the depletion of mtDNA. Although mtDNA was completely depleted after a long exposure of HeLa cells to ethidium bromide, its nuclear genes may be affected at a high frequency. Thus, we used a cybrid clone, Ft2-11, that had been obtained by the intercellular transfer of wild-type mitochondria into EB8 cells as a control instead of parental HeLa cells. This procedure, cell fusion between enucleated cells (mitochondrion donor) and EB8 cells, would cause no damage to the nuclear genes.

On comparing the mRNA isolated from EB8 cells with that of control cells by differential display, we found three genes whose expression was higher in EB8 cells. Two of them were the apurinic/apyrimidinic endonuclease I (APE1/HAP1) (Demple et al., 1991) and DNA ligase III genes (Wei et al., 1995). These gene products are located in mitochondria as well as the nucleus and are involved in DNA repair. Thus, it is reasonable to assume that the mitochondrial repair system responds to the depletion of mtDNA.

The third gene product, named MIDAS here, was identical to a Golgi protein, GPP34. The nucleotide sequence of *MIDAS/GPP34* is conserved from yeast to human (Bell et al., 2001; Wu et al., 2000). Its yeast *Saccharomyces cerevisiae* homolog (YDR372c) has been deleted revealing that the gene is not essential for viability (Winzeler et al., 1999; Bidlingmaier and Snyder, 2002). Although a mutation in the YDR372c gene revealed a phenotype with an abnormal budding (Bidlingmaier and Snyder, 2002) and aberrant in protein-vacuolar targeting (Bonangelino et al., 2002), the molecular function of the gene product remains unknown. Genetic analysis showed that there are genetic interactions between YDR372c and intracellular protein-transport factors (RIC1 and YPT6) (Tong et al., 2004). As MIDAS has a leucine-zipper motif (supplementary material Fig. S1), it may interact with a protein involved in intracellular protein transport through this motif.

In most mitochondrial diseases, mutant mtDNA coexists with wild-type mtDNA at various ratios in a heteroplasmic manner and exhibits a cognate pathological phenotype in a threshold-dependent manner. COX-deficient cells have abundant mutant mtDNA, whereas COX-positive cells have a small amount of mutant mtDNA. MIDAS was shown to be more abundant in muscle cells with no COX activity in patients with mitochondrial diseases. This finding indicates that the enhanced expression of MIDAS occurs not only in HeLa cells lacking mtDNA, but also in muscle cells with pathogenic mutant mtDNAs, regardless of point mutations or deletions of mtDNA. MIDAS has putative ATF-1 binding sites and the upregulated expression by EWS/ATF-1 chimeric transcription factor was revealed (Jishage et al., 2003). When mitochondrial dysfunction occurs, the expression of MIDAS may be activated by CREB/ATF-1 family transcription factors.

A previous report (Bell et al., 2001) indicated that GPP34 colocalizes only with Golgi, but not mitochondria. When we used the method they described (Bell et al., 2001) with permeabilization pretreatment after fixation, anti-MIDAS antibody stained only the Golgi apparatus (Fig. 3D,E). On the other hand, immunostaining clearly showed that MIDAS colocalized with both mitochondria and the Golgi apparatus when the cells were subjected to the acetate/ethanol pretreatment to permeabilize the mitochondrial membranes. An outer membrane protein (Tom 20) did not require the permeabilization procedure for staining, but the acetate/ethanol procedure was essential for the proteins located inside mitochondria such as cytochrome c, Hsp60 and SDH70 (Fig. 3C and supplementary material Fig. S3). Thus, the discrepancy is fully explained by the difference in the permeabilization method used (Fig. 3). The present result is consistent with the result of a sub-organellar fractionation experiment that showed that MIDAS is present in the intermembrane space. Thus, it is concluded that the antibody against MIDAS/GPP34 cannot access the mitochondrial MIDAS without the permeabilization pretreatment. As MIDAS lacks typical sequences that could target mitochondria or the Golgi apparatus, it is unknown how it is directed to the respective organelle.

As MIDAS/GPP34 has an isoform, named GPP34R, one may target mitochondria and the other may target the Golgi apparatus. However, this is unlikely because GPP34R was expressed at a level less than 2% of that of MIDAS in HeLa cells. This small amount cannot account for the relative amount of the protein located in the Golgi apparatus. In addition, we performed a crucial experiment. As the fusion protein comprising Myc-tag and the N-terminus of MIDAS targets only Golgi, the N-terminal region may be responsible for targeting mitochondria. In contrast, an alternative fusion protein with Myc-tag at the C-terminus of MIDAS targets mitochondria. This experiment suggests that the single molecule has the potential to localize to two distinct organelles. Further experiments will reveal which location of MIDAS contributes to its distribution.

Mitochondria gathered around the nucleus in MIDAS-expressing transfectants. As mitochondria often gather around the nucleus in sick cells regardless of internal or external conditions, it may be that toxicity of MIDAS forces mitochondria to concentrate around the nucleus by affecting the cytoskeletal structure. However, no abnormal cytoskeletal structure was found in MIDAS-expressing transfectants (supplementary material Fig. S6). Thus, the mitochondrial accumulation was not due to abnormality of the cytoskeleton. The mitochondrial biogenesis occurs near the nucleus and fresh mitochondria are transported to peripheral areas (Yaffe, 1999). Thus, newly synthesized mitochondria seem to be concentrated around the nucleus and then the excess mitochondria may push up the nucleus as seen in Fig. 5B and Fig. 6D, second panel.

A transcriptional coactivator PGC-1 enhances the expression of many mitochondrial proteins by activating several transcription factors, such as NRF-1, NRF-2, Sp1, YY1, CREB and MEF-2/E-box (Scarpulla, 2002). Recognition sites for NRF-1, NRF-2 and Sp1 are common to most nuclear genes encoding components involved in mitochondrial respiration, transcription and replication (Scarpulla, 2002). However, it is unknown how PGC-1 contributes to the increase in mitochondrial lipids. In addition, there has been no report that PGC-1 is expressed in response to mitochondrial dysfunction or damage. MIDAS seems to accumulate mitochondria by an

alternative pathway from PGC-1 because MIDAS did not enhance mitochondrial transcription (Fig. 7C).

As mitochondria dynamically repeat fusion and fission, it is difficult to clarify their number (Griparic and van der Bliek, 2001; Westermann, 2002). In this study, we thus paid attention to the total mass of mitochondria. Three-dimensional imaging revealed a change in the total mass of mitochondria. The increase was 1.6-fold, which agrees with the increase in strength of the fluorescence of MitoTracker Red and MitoTracker Green in MIDAS-expressing transfectants. This increase is not so small because mitochondria occupy more than 20% of the total volume of the cytoplasm in HeLa cells. When the downregulation and upregulation of MIDAS were compared, the total mass was found to vary more than 2.3-fold from 15% to 35% of the total cytoplasm of HeLa cells. Thus, MIDAS dramatically regulates the total mitochondrial mass.

Mitochondria are often swollen pathogenically or by an increase of cytosolic Ca^{2+}. It may be that the mitochondria are simply swollen owing to the expression of MIDAS. However, this is unlikely for the following reasons. First, the ratio of the intensity in red to the intensity in green was the same in all the cells examined, indicating that MIDAS does not exert any influence on membrane potential (Fig. 6C). Although MIDAS-expressing cells have lower concentrations of mitochondrial protein per volume than controls (Fig. 7C), the levels seem high enough for membrane potential. Second, the downregulation of MIDAS conversely decreased the total mass of mitochondria. Third, mitochondria appear intact morphologically, being independent of the up- or downregulation of MIDAS (Fig. 5C). Finally, it is crucial that the amount of cardiolipin varied depending upon the amount of MIDAS and that the extent of the change was well correlated with the total mass of mitochondria that was revealed by three-dimensional imaging. Cardiolipin is a mitochondrion-specific lipid but accounts for only 20% of mitochondrial lipids. This suggests that not only the amount of cardiolipin but also the total amount of mitochondrial lipids is changed by MIDAS. Taken together, it is concluded that total mitochondrial mass is regulated by MIDAS through the biogenesis of mitochondrial lipids.

The molecular mechanism by which the MIDAS protein increases production of cardiolipin is unknown. A detailed analysis of the *MIDAS* gene and the function of MIDAS should provide insight into the molecular mechanism by which mitochondrial dysfunction is sensed to increase mitochondria. The fact that MIDAS is colocalized with both mitochondria and the Golgi apparatus may be a key to answering the question of how lipids contribute to mitochondrial accumulation.

We thank K. Mihara of Kyushu University for the gift of anti-Tom20 and anti-Tom40 antibodies, I. Ohsawa and T. Kanamori for helpful advice and K. Yamagata for technical assistance.

References

Amuthan, G., Biswas, G., Zhang, S. Y., Klein-Szanto, A., Vijayasarathy, C. and Avadhani, N. G. (2001). Mitochondria-to-nucleus stress signaling induces phenotypic changes, tumor progression and cell invasion. *EMBO J.* **20**, 1910-1920.

Asoh, S., Mori, T., Hayashi, J. and Ohta, S. (1996). Expression of the apoptosis-mediator Fas is enhanced by dysfunctional mitochondria. *J. Biochem. (Tokyo)* **120**, 600-607.

Attardi, G. and Schatz, G. (1988). Biogenesis of mitochondria. *Annu. Rev. Cell Biol.* **4**, 289-333.

Bell, A. W., Ward, M. A., Blackstock, W. P., Freeman, H. N., Choudhary, J. S., Lewis, A. P., Chotai, D., Fazel, A., Gushue, J. N., Paiement, J. et al. (2001). Proteomics characterization of abundant Golgi membrane proteins. *J. Biol. Chem.* **276**, 5152-5165.

Bereiter-Hahn, J. and Voth, M. (1994). Dynamics of mitochondria in living cells: shape changes, dislocations, fusion and fission of mitochondria. *Microsc. Res. Tech.* **27**, 198-219.

Bidlingmaier, S. and Snyder, M. (2002). Large-scale identification of genes important for apical growth in *Saccharomyces cerevisiae* by directed allele replacement technology (DART) screening. *Funct. Integr. Genomics* **1**, 345-356.

Biswas, G., Adebanjo, O. A., Freedman, B. D., Anandatheerthavarada, H. K., Vijayasarathy, C., Zaidi, M., Kotlikoff, M. and Avadhani, N. G. (1999). Retrograde Ca^{2+} signaling in C2C12 skeletal myocytes in response to mitochondrial genetic and metabolic stress: a novel mode of inter-organelle crosstalk. *EMBO J.* **18**, 522-533.

Bonangelino, C. J., Chavez, E. M. and Bonifacino, J. S. (2002). Genomic screen for vacuolar protein sorting genes in *Saccharomyces cerevisiae*. *Mol. Biol. Cell* **13**, 2486-2501.

Brunk, C. F. (1981). Mitochondrial proliferation during myogenesis. *Exp. Cell Res.* **136**, 305-309.

Collins, T. J., Berridge, M. J., Lipp, P. and Bootman, M. D. (2002). Mitochondria are morphologically and functionally heterogeneous within cells. *EMBO J.* **21**, 1616-1627.

Cortopassi, G. A. and Wong, A. (1999). Mitochondria in organismal aging and degeneration. *Biochim. Biophys. Acta* **1410**, 183-193.

Demple, B., Herman, T. and Chen, D. S. (1991). Cloning and expression of APE, the cDNA encoding the major human apurinic endonuclease: definition of a family of DNA repair enzymes. *Proc. Natl. Acad. Sci. USA* **88**, 11450-11454.

Dubowitz, V. (1985). Histological and histochemical stains and reactions. In *Muscle Biopsy: a practical approach*, 2nd edn, (ed. V. Dubowitz), pp. 19-40. London: Balliere Tindall.

Engel, W. K. and Cunningham, G. G. (1963). Rapid examination of muscle tissue. An improved trichrome method for fresh-frozen biopsy sections. *Neurology* **13**, 919-926.

Erlich, R., Gleeson, P. A., Campbell, P., Dietzsch, E. and Toh, B. H. (1996). Molecular characterization of *trans*-Golgi p230. A human peripheral membrane protein encoded by a gene on chromosome 6p12-22 contains extensive coiled-coil alpha-helical domains and a granin motif. *J. Biol. Chem.* **271**, 8328-8337.

Folch, J., Lees, M. and Sloane Stanley, G. H. (1957). A simple method for the isolation and purification of total lipides from animal tissues. *J. Biol. Chem.* **226**, 497-509.

Garesse, R. and Vallejo, C. G. (2001). Animal mitochondrial biogenesis and function: a regulatory cross-talk between two genomes. *Gene* **263**, 1-16.

Goglia, F., Moreno, M. and Lanni, A. (1999). Action of thyroid hormones at the cellular level: the mitochondrial target. *FEBS Lett.* **452**, 115-120.

Goto, Y., Nonaka, I. and Horai, S. (1990). A mutation in the $tRNA^{Leu(UUR)}$ gene associated with the MELAS subgroup of mitochondrial encephalomyopathies. *Nature* **348**, 651-653.

Green, D. R. and Kroemer, G. (2004). The pathophysiology of mitochondrial cell death. *Science* **305**, 626-629.

Griparic, L. and van der Bliek, A. M. (2001). The many shapes of mitochondrial membranes. *Traffic* **2**, 235-244.

Hansson, A., Hance, N., Dufour, E., Rantanen, A., Hultenby, K., Clayton, D. A., Wibom, R. and Larsson, N. G. (2004). A switch in metabolism precedes increased mitochondrial biogenesis in respiratory chain-deficient mouse hearts. *Proc. Natl. Acad. Sci. USA* **101**, 3136-3141.

Hasegawa, H., Matsuoka, T., Goto, Y. and Nonaka, I. (1991). Strongly succinate dehydrogenase-reactive blood vessels in muscles from patients with mitochondrial myopathy, encephalopathy, lactic acidosis and stroke-like episodes. *Ann. Neurol.* **29**, 601-605.

Hayashi, J., Ohta, S., Kikuchi, A., Takemitsu, M., Goto, Y. and Nonaka, I. (1991). Introduction of disease-related mitochondrial DNA deletions into HeLa cells lacking mitochondrial DNA results in mitochondrial dysfunction. *Proc. Natl. Acad. Sci. USA* **88**, 10614-10618.

Hayashi, J., Ohta, S., Kagawa, Y., Kondo, H., Kaneda, H., Yonekawa, H., Takai, D. and Miyabayashi, S. (1994). Nuclear but not mitochondrial genome involvement in human age-related mitochondrial dysfunction. Functional integrity of mitochondrial DNA from aged subjects. *J. Biol. Chem.* **269**, 6878-6883.

Holt, I. J., Harding, A. E. and Morgan-Hughes, J. A. (1988). Deletions of muscle mitochondrial DNA in patients with mitochondrial myopathies. *Nature* **331**, 717-719.

Jishage, M., Fujino, T., Yamazaki, Y., Kuroda, H. and Nakamura, T. (2003). Identification of target genes for EWS/ATF-1 chimeric transcription factor. *Oncogene* **22**, 41-49.

Kanamori, T., Nishimaki, K., Asoh, S., Ishibashi, Y., Takata, I., Kuwabara, T., Taira, K., Yamaguchi, H., Sugihara, S., Yamazaki, T. et al. (2003). Truncated product of the bifunctional *DLST* gene involved in biogenesis of the respiratory chain. *EMBO J.* **22**, 2913-2923.

Kang, D. and Hamasaki, N. (2002). Maintenance of mitochondrial DNA integrity: repair and degradation. *Curr. Genet.* **41**, 311-322.

Kawahara, H., Houdou, S. and Inoue, T. (1991). Scanning electron microscopic observations on muscle cells of experimental mitochondrial myopathy produced by 2, 4-dinitrophenol. *J. Submicrosc. Cytol. Pathol.* **23**, 397-403.

Klaus, S., Casteilla, L., Bouillaud, F. and Ricquier, D. (1991). The uncoupling protein UCP: a membraneous mitochondrial ion carrier exclusively expressed in brown adipose tissue. *Int. J. Biochem.* **23**, 791-801.

Kobayashi, Y., Momoi, M. Y., Tominaga, K., Momoi, T., Nihei, K., Yanagisawa, M., Kagawa, Y. and Ohta, S. (1990). A point mutation in the mitochondrial $tRNA^{Leu(UUR)}$ gene in MELAS (mitochondrial myopathy, encephalopathy, lactic acidosis and stroke-like episodes). *Biochem. Biophys. Res. Commun.* **173**, 816-822.

Kobayashi, Y., Momoi, M. Y., Tominaga, K., Shimoizumi, H., Nihei, K., Yanagisawa, M., Kagawa, Y. and Ohta, S. (1991). Respiration-deficient cells are caused by a single point mutation in the mitochondrial $tRNA^{Leu(UUR)}$ gene in mitochondrial myopathy, encephalopathy, lactic acidosis and strokelike episodes (MELAS). *Am. J. Hum. Genet.* **49**, 590-599.

Kowaltowski, A. J. and Vercesi, A. E. (1999). Mitochondrial damage induced by conditions of oxidative stress. *Free Radic. Biol. Med.* **26**, 463-471.

Kroemer, G. and Reed, J. C. (2000). Mitochondrial control of cell death. *Nat. Med.* **6**, 513-519.

Liang, P. and Pardee, A. B. (1992). Differential display of eukaryotic messenger RNA by means of the polymerase chain reaction. *Science* **257**, 967-971.

Lightowlers, R. N., Chinnery, P. F., Turnbull, D. M. and Howell, N. (1997). Mammalian mitochondrial genetics: heredity, heteroplasmy and disease. *Trends Genet.* **13**, 450-455.

Melov, S. (2000). Mitochondrial oxidative stress. Physiologic consequences and potential for a role in aging. *Ann. New York Acad. Sci.* **908**, 219-225.

Moraes, C. T., Ricci, E., Bonilla, E., DiMauro, S. and Schon, E. A. (1992). The mitochondrial $tRNA^{Leu(UUR)}$ mutation in mitochondrial encephalomyopathy, lactic acidosis and strokelike episodes (MELAS): genetic, biochemical and morphological correlations in skeletal muscle. *Am. J. Hum. Genet.* **50**, 934-949.

Moyes, C. D., Mathieu-Costello, O. A., Tsuchiya, N., Filburn, C. and Hansford, R. G. (1997). Mitochondrial biogenesis during cellular differentiation. *Am. J. Physiol.* **272**, C1345-C1351.

Muller-Hocker, J., Pongratz, D. and Hubner, G. (1986). Activation of mitochondrial ATPase as evidence of loosely coupled oxidative phosphorylation in various skeletal muscle disorders. A histochemical fine-structural study. *J. Neurol. Sci.* **74**, 199-213.

Munro, S. and Pelham, H. R. (1987). A C-terminal signal prevents secretion of luminal ER proteins. *Cell* **48**, 899-907.

Nisoli, E., Clementi, E., Paolucci, C., Cozzi, V., Tonello, C., Sciorati, C., Bracale, R., Valerio, A., Francolini, M., Moncada, S. et al. (2003). Mitochondrial biogenesis in mammals: the role of endogenous nitric oxide. *Science* **299**, 896-899.

Nisoli, E., Falcone, S., Tonello, C., Cozzi, V., Palomba, L., Fiorani, M., Pisconti, A., Brunelli, S., Cardile, A., Francolini, M. et al. (2004). Mitochondrial biogenesis by NO yields functionally active mitochondria in mammals. *Proc. Natl. Acad. Sci. USA* **101**, 16507-16512.

Ohta, S. (2003). A multi-functional organelle mitochondrion is involved in cell death, proliferation and disease. *Curr. Med. Chem.* **10**, 2485-2494.

Pfanner, N. and Geissler, A. (2001). Versatility of the mitochondrial protein import machinery. *Nat. Rev. Mol. Cell. Biol.* **2**, 339-349.

Scarpulla, R. C. (2002). Nuclear activators and coactivators in mammalian mitochondrial biogenesis. *Biochim. Biophys. Acta* **1576**, 1-14.

Schon, E. A. (2000). Mitochondrial genetics and disease. *Trends Biochem. Sci.* **25**, 555-560.

Shoubridge, E. A., Karpati, G. and Hastings, K. E. (1990). Deletion mutants are functionally dominant over wild-type mitochondrial genomes in skeletal muscle fiber segments in mitochondrial disease. *Cell* **62**, 43-49.

Tong, A. H., Lesage, G., Bader, G. D., Ding, H., Xu, H., Xin, X., Young, J., Berriz, G. F., Brost, R. L., Chang, M. et al. (2004). Global mapping of the yeast genetic interaction network. *Science* **303**, 808-813.

Trounce, I. A., Kim, Y. L., Jun, A. S. and Wallace, D. E. (1996). Assessment of mitochondrial oxidative phosphorylation in patient muscle biopsies, lymphoblasts and transmitochondrial cell lines. *Methods Enzymol.* **264**, 484-509.

Vorobjev, I. A. and Zorov, D. B. (1983). Diazepam inhibits cell respiration and induces fragmentation of mitochondrial reticulum. *FEBS Lett.* **163**, 311-314.

Wallace, D. C. (1999). Mitochondrial diseases in man and mouse. *Science* **283**, 1482-1488.

Weber, K., Ridderskamp, D., Alfert, M., Hoyer, S. and Wiesner, R. J. (2002). Cultivation in glucose-deprived medium stimulates mitochondrial biogenesis and oxidative metabolism in HepG2 hepatoma cells. *Biol. Chem.* **383**, 283-290.

Wei, Y. F., Robins, P., Carter, K., Caldecott, K., Pappin, D. J., Yu, G. L., Wang, R. P., Shell, B. K., Nash, R. A., Schar, P. et al. (1995). Molecular cloning and expression of human cDNAs encoding a novel DNA ligase IV and DNA ligase III, an enzyme active in DNA repair and recombination. *Mol. Cell. Biol.* **15**, 3206-3216.

Westermann, B. (2002). Merging mitochondria matters: Cellular role and molecular machinery of mitochondrial fusion. *EMBO Rep.* **3**, 527-531.

Winzeler, E. A., Shoemaker, D. D., Astromoff, A., Liang, H., Anderson, K., Andre, B., Bangham, R., Benito, R., Boeke, J. D., Bussey, H. et al. (1999). Functional characterization of the *S. cerevisiae* genome by gene deletion and parallel analysis. *Science* **285**, 901-906.

Wu, C. C., Taylor, R. S., Lane, D. R., Ladinsky, M. S., Weisz, J. A. and Howell, K. E. (2000). GMx33: a novel family of *trans*-Golgi proteins identified by proteomics. *Traffic* **1**, 963-975.

Yaffe, M. P. (1999). The machinery of mitochondrial inheritance and behavior. *Science* **283**, 1493-1497.

Zeller, R. (1998). Preparation of cells and tissues for fluorescence microscopy. In *Cells: A Laboratory Manual. Volume 3 Subcellular localization of genes and their products.* (ed. D. L. Spector, R. D. Goldman and L. A. Leinwand), pp. 98.01-98.20. New York: Cold Spring Harbor Laboratory Press.

Vascular Involvement in a Patient with Mitochondrial Myopathy, Encephalopathy, Lactic Acidosis, and Stroke-Like Episodes

NOBUYUKI TAKAHASHI, MD, PHD; TOSHIO SHIMADA, MD, PHD; YO MURAKAMI, MD, PHD; HARUMI KATOH, MD, PHD; NOBUYUKI OYAKE, MD; YUTAKA ISHIBASHI, MD, PHD; ICHIZO NISHINO, MD, PHD; IKUYA NONAKA, MD, PHD; YU-ICHI GOTO, MD, PHD

ABSTRACT: A 26-year-old man with mitochondrial myopathy, encephalopathy, lactic acidosis, and stroke-like episodes (MELAS) was admitted to our hospital for further cardiovascular examination. A muscle biopsy demonstrated strongly succinate dehydrogenase–reactive blood vessels. Pulse wave contour analysis revealed that both capacitive and oscillatory compliance were markedly reduced in this patient compared with 45 normal age-matched control subjects. Hepatocyte growth factor was remarkably elevated in this patient over that of 10 normal control subjects. These findings suggest that a MELAS patient has not only pathologic but also functional vascular involvement. If so, patients with MELAS need systemic vascular assessment. **KEY INDEXING TERMS:** MELAS; Vascular involvement; Pulse wave contour analysis; Hepatocyte growth factor. **[Am J Med Sci 2005;329(5):265–266.]**

Mitochondria are intracellular organelles that produce adenosine triphosphate and contain a small number of genes transmitted only from the mother. Most of these genes are closely related to the energy-producing process. A mitochondrial gene abnormality may therefore lead to fatal organ failure, particularly in mitochondria-rich organs such as the brain and the heart, and in the smooth muscles.

MELAS, or mitochondrial myopathy, encephalopathy, lactic acidosis, and stroke-like episodes, was first described by Pavlakis et al[1] as a new distinct clinical entity among the mitochondrial encephalomyopathies.

In patients with MELAS, preferential vascular involvement is believed to be responsible for the strikingly episodic nature of its clinical manifestations, as demonstrated in previous studies of mitochondrial abnormalities in arteries of the brain.[2] Additionally, Sakuta and Nonaka[3] found abnormal mitochondria in the smooth muscle cells of the small arteries in muscle biopsy specimens from MELAS patients. Vascular involvement is not confined to the central nervous system; it may also be present in a number of organs in patients with MELAS.

To our knowledge, however, there have been no reports of functional abnormalities arising from vascular involvement in patients with MELAS. We believe this is the first case study of both pathologic and functional vascular abnormalities in a patient with MELAS.

Case Report

A 26-year-old man with MELAS was admitted to our university hospital for further cardiovascular examination. At the age of 18, the patient had a generalized convulsion and was diagnosed with insulin-dependent diabetes mellitus. At the age of 24, a mitochondrial DNA mutation (A3243G) known to be specific for MELAS[4] was identified in his leukocytes, and he was diagnosed with MELAS. His mother, sister, and grandmother had suffered from insulin-dependent diabetes mellitus, and the A3243G leukocyte mutation was also identified in his mother. At the age of 26, the patient was admitted to another hospital because of drowsiness, convulsion, right hemiplegia, and aphasia. Two months later, he was referred to our hospital for further cardiovascular examination.

Physical examination showed him to be of short stature (152.2 cm tall) and weighing 34.9 kg. He was normotensive and had no arteriosclerosis obliterans. He displayed severe neurosensory hearing disturbance and mental retardation. A chest radiograph revealed neither cardiomegaly nor pulmonary congestion, and both the electrocardiogram and the echocardiogram showed no abnormal findings.

Muscle biopsy specimens obtained from the left quadriceps

From the Division of Cardiovascular Medicine, Department of Internal Medicine, Shimane University Faculty of Medicine, Shimane, Japan (NT, TS, YM, HK, NO, YI); and from the Department of Neuromuscular Research (INi, INo) and the Department of Mental Retardation and Birth Defect Research (YG), National Institute of Neuroscience, National Center of Neurology and Psychiatry, Tokyo, Japan.

Submitted September 10, 2004; accepted December 6, 2004.

Correspondence: Toshio Shimada, MD, PhD, Division of Cardiovascular Medicine, Department of Internal Medicine, Shimane University Faculty of Medicine, 89-1 Enya-cho, Izumo City, Shimane 693-8501, Japan (E-mail address: tshimada@med.shimane-u.ac.jp).

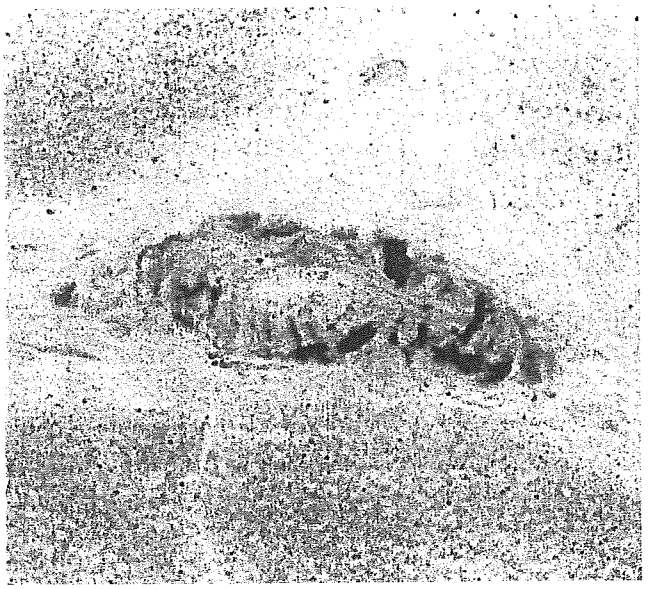

Figure 1. Strongly succinate dehydrogenase-reactive blood vessels in the muscle biopsy obtained from the left quadriceps femoris.

femoris demonstrated strongly succinate dehydrogenase-reactive blood vessels, which can be useful for supporting or making a diagnosis of MELAS[5] (Figure 1). The mutation rate for mitochondria in the patient's skeletal muscle was 78% according to the Taq-Man method. Pulse wave contour analysis, which can be useful for screening vascular disease,[6] revealed markedly lower compliance, both capacitive and oscillatory, in this patient than in 45 normal control subjects his age (capacitive compliance, 7.7 versus 15.6 ± 3.3 mL/mm Hg ×10; oscillatory compliance, 3.7 versus 8.2 ± 2.7 mL/mm Hg ×100). Hepatocyte growth factor (HGF), which has recently been considered as a possible index of the severity of vascular involvement in patients with hypertension,[7,8] was found to be remarkably elevated in this patient, compared with 10 normal control subjects (0.29 versus 0.05 ± 0.03 ng/mL).

Discussion

Vascular involvement in patients with MELAS has already been investigated in several studies,[2,3,5] and it is believed that vascular abnormalities may be responsible for the occasional occurrence of transient cerebral ischemia that causes stroke-like episodes and progressive mental deterioration in patients with MELAS. Vascular involvement in mitochondrial myopathy also extends to the whole body.[5] To the best of our knowledge, however, there have been no reports on vascular dysfunction in patients with MELAS.

Cohn et al[6] recently developed noninvasive pulse wave analysis for estimating human vascular properties. We applied this technique to estimate vascular dysfunction in this patient and found both capacitive and oscillatory arterial compliance to be significantly reduced in this patient compared with 45 normal control subjects.

Additionally, HGF is a pleiotropic polypeptide growth factor with abundant biologic activities in a variety of epithelial tissues.[9] Endothelial dysfunction in hypertensive patients is well known,[10] and serum HGF has been considered as a possible index of endothelial dysfunction in patients with hypertension.[7,8] This patient's serum HGF was remarkably elevated compared with that of 10 normal control subjects his age. HGF may also be an indicator of endothelial dysfunction in patients with MELAS.

A previous study demonstrated that oscillatory compliance is reduced in patients with non-insulin-dependent diabetes mellitus.[11] Morishita et al[12] demonstrated, however, that HGF production significantly decreases in accordance with the severity of diabetes mellitus. The elevated serum HGF level and reduced capacitive and oscillatory compliance of this patient may therefore reflect the mitochondrial abnormalities of MELAS rather than diabetes mellitus itself.

These results suggest that patients with MELAS have abnormal vascular dysfunction. Systemic vascular assessment may therefore be needed in future treatment of patients with MELAS.

References

1. **Pavlakis SG, Phillips PC, Dimauro S, et al.** Mitochondrial myopathy, encephalopathy, lactic acidosis, and stroke-like episodes: a distinctive clinical syndrome. Ann Neurol 1984;16:481–8.
2. **Ohama E, Ohama S, Ikuta F, et al.** Mitochondrial angiopathy in cerebral blood vessels of mitochondrial encephalopathy. Acta Neuropathol 1987;74:226–33.
3. **Sakuta R, Nonaka I.** Vascular involvement in mitochondrial myopathy. Ann Neurol 1989;25:594–601.
4. **Goto Y, Nonaka I, Horai S.** A mutation in the tRNALeu(UUR) gene associated with the MELAS subgroup of mitochondrial encephalomyopathies. Nature 1990;348:651–3.
5. **Hasegawa H, Matsuoka T, Goto Y, et al.** Strongly succinate dehydrogenase-reactive blood vessels in muscles from patients with mitochondrial myopathy, encephalopathy, lactic acidosis, and stroke-like episodes. Ann Neurol 1991;29:601–5.
6. **Cohn J, Finkelstein S, McVeigh G, et al.** Noninvasive pulse wave analysis for the early detection of vascular disease. Hypertension 1995;26:503–8.
7. **Nakamura S, Moriguchi A, Morishita R, et al.** A novel vascular modulator, hepatocyte growth factor (HGF), as a potential index of the severity of hypertension. Biochem Biophys Res Com 1998;242:238–43.
8. **Morishita R, Nakamura S, Hayashi S, et al.** Contribution of a vascular modulator, hepatocyte growth factor (HGF), to the pathogenesis of cardiovascular disease. J Atheroscler Thromb 1998;4:128–34.
9. **Boros P, Miller C.** Hepatocyte growth factor: a multifunctional cytokine. Lancet 1995;345:293–5.
10. **Panza JA, Quyyumi AA, Brush JE Jr, et al.** Abnormal endothelium-dependent vascular relaxation in patients with essential hypertension. N Engl J Med 1990;323:22–7.
11. **McVeigh G, Brennan G, Hayes R, et al.** Vascular abnormalities in non-insulin-dependent diabetes mellitus identified by arterial waveform analysis. Am J Med 1993;95:424–30.
12. **Morishita R, Nakamura S, Nakamura Y, et al.** Potential role of an endothelium-specific growth factor, hepatocyte growth factor, on endothelial damage in diabetes. Diabetes 1997;46:138–42.

蛋白質核酸酵素

PNE

PROTEIN,
NUCLEIC ACID
AND ENZYME

別刷

「蛋白質 核酸 酵素」編集部
共立出版株式会社
〒112-8700　東京都文京区小日向 4-6-19
Tel.03-3947-2515　FAX 03-3944-8182
E-mail：pne@kyoritsu-pub.co.jp
http://www.kyoritsu-pub.co.jp/

3. 哺乳類ミトコンドリアゲノムの変異と疾患

ミトコンドリアDNA異常によるヒト疾患

後藤雄一

ミトコンドリアDNA（mtDNA）異常により種々の症状が出現することが知られている．とくにエネルギーを多量に必要とする組織・臓器である中枢神経，骨格筋，心臓などに症状が出やすい．mtDNAの異常には，量的異常と質的異常がある．量的異常とはmtDNA欠乏症候群であり，乳児に発症するものや薬剤性のものが知られている．質的異常には，欠失/重複と点変異があり，種々の臨床病型の原因になっている．mtDNAの欠乏や多重欠失の場合は，mtDNAの複製や維持にかかわる核DNA上の遺伝子変異が1次的病因である．

▶▶KEY WORDS：ミトコンドリア病　mtDNA欠乏症候群　ヘテロプラスミー

■はじめに■

ミトコンドリアの機能異常によって起こるヒトの病気を「ミトコンドリア病」と称している．ミトコンドリアは成熟赤血球以外の全身のあらゆる細胞に存在しており，よってその機能異常は種々の症状をひき起こす．とくに，エネルギーを大量に消費する細胞，組織ではその障害が現れやすく，中枢神経，骨格筋，心筋などにおける症状が前景にでることが多いため，以前はミトコンドリア脳筋症ともよばれていた．ミトコンドリアの機能障害が，細胞レベル，組織レベル，臓器レベルで現れる表現型は異なり，臨床症状としてとらえられるのは組織・臓器レベルの表現型である．たとえば，脳卒中，てんかん，精神症状，夜盲，運動失調，心筋症，易疲労感，糖尿病など，まさにあらゆる症状と関係があるといってよい．一方で，脳卒中や糖尿病という症状はミトコンドリア機能異常以外の原因でも起こりうるので，それがミトコンドリア病であるというためには，患者におけるミトコンドリア機能異常を証明しなくてはならない．その意味で，細胞レベルのミトコンドリア異常を病理学的，生化学的，分子遺伝学的に明らかにすることが診断の根拠となる．ミトコンドリア病においては，mtDNA異常や核DNA上の遺伝子変異の検索は病因を知るための重要な検査であるが，それだけでは診断を誤る可能性があり，病理学的，生化学的検査を合わせて総合的に診断することが肝要である（図1）．

I. mtDNAの特徴がそのまま病気の特徴に反映する

mtDNAは環状二本鎖のDNAで，ヒトでは16,568塩基からなっている．コードされている蛋白質はすべて電子伝達系酵素のサブユニットであり，ほかに2個のリボソームRNA遺伝子，22個の転移RNA遺伝子がコードされている．核DNAと特徴的に異なることは，mtDNAは1細胞に数百から数千個存在していることである．それは，1個のミトコンドリアに5～10個のmtDNAが存在し，1細胞に数十から数百のミトコンドリアが存在しているからである．1細胞に1対（2本）のDNAセットしかもたない核DNAとは著しく異なる．

実際のミトコンドリア病患者でみつかる変異mtDNAは，多くの場合正常mtDNAと共存している（ヘテロプラスミーという）．すなわち，細胞や組織ごとで，変異mtDNAと正常mtDNAの比率が異なるのである．ただし，変異mtDNAばかり（ホモプラスミーという）のこともあり，後述するLeigh脳症に認められる8993変異やLeber視神経萎縮症に認められる11778変異の場合などである．

興味深いことに，変異mtDNAが存在すれば，ミトコンドリア機能異常を必ずひき起こすわけではない．細胞のなかの変異mtDNAの比率が閾値以上にならないと機能障害が起こらない．これを閾値効果といい，したがって検査で変異mtDNAが検出されたからといって，病気と断定してはいけない．

Yu-ichi Goto，国立精神・神経センター神経研究所　E-mail：goto@ncnp.go.jp　www.ncnp.go.jp/nin/guide/r2/index.html
Pathogenic mutations in human mtDNA and their phenotypes

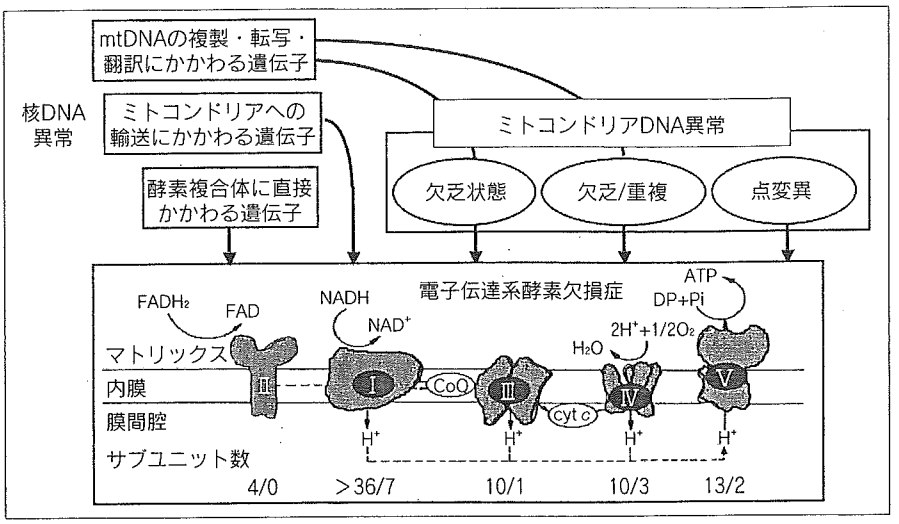

図1　ミトコンドリア病の病因

ミトコンドリア病の病因には，核DNA異常とmtDNA異常がある．mtDNA異常には，欠乏状態，欠失/重複，点変異がある．いずれも電子伝達系酵素欠損症を惹起し，病気を発症する．核DNA異常のなかで，酵素複合体にかかわる遺伝子（サブユニット遺伝子，集合にかかわる因子の遺伝子），ミトコンドリア内への輸送にかかわる因子の遺伝子は，直接，電子伝達系酵素活性に影響を与える．しかし，核DNA上にコードされている遺伝子でも，mtDNAの複製・転写・翻訳にかかわる遺伝子は，mtDNAの欠乏状態や多重欠失をひき起こしてから，電子伝達系酵素欠損症を起こすと考えられる．
電子伝達系酵素複合体の下に記載されている数字は，核DNA/mtDNAにコードされているサブユニットの数を表している．

ヘテロプラスミーの性質は，細胞や組織ごとの多様性をひき起こす．変異mtDNAは患者のある組織では検出できるのに，別の組織では検出できない可能性があり，実際mtDNAの欠失は，骨格筋では検出できるのに血液細胞や線維芽細胞では検出できないことがある．また，点変異の場合でも，組織ごとで変異mtDNAの比率が大きく異なることがある．したがって，mtDNA検査の対象は罹患臓器にするのが原則である．

しかし，中枢神経を生検することは実際的でなく，通常は骨格筋を対象とする．その理由は，剖検例などの検討で，欠失でも点変異でも変異mtDNAの比率がもっとも高いのが骨格筋であり，骨格筋は同時に病理学的にも生化学的にも検査が可能であるので，総合的に結果を判断できるからである．

II. おもなmtDNA異常と表現型

1. mtDNAの量的異常（欠乏状態）

1細胞中に数千コピー存在しているmtDNAの量が減少することで病的状態が起こる．mtDNAの欠乏状態を検出するには，核DNA上に存在しているリボソームRNAをコードしている領域（ゲノム上に繰返し配列が数百コピーあるといわれている）を内部標準として，それに対してどの程度の量で存在しているかをサザン法や定量的PCR法で計測する．

この欠乏状態は，遺伝性と薬剤性の場合が知られている．遺伝性としては，最初に記載された腎不全や肝不全を伴う筋症以外に[1]，消化器症状と白質変性を特徴とするMNGIE（mitochondrial neurogastrointestinal encephalomyopathy），乳児期発症のミオパチータイプなどが知られている（表1）．MNGIEではチミジンホスホリラーゼ1（TP1）[2]，乳児期発症のミオパチータイプではチミジンキナーゼ2（TK2）[3]，デオキシグアノシンキナーゼ（dGK）[4]の遺伝子変異によって起こることが判明している．一方，薬剤性としては，AIDSの治療薬の一つであるAZTによるものがもっとも有名である[5]．AZTやddC（ジデオキシシトシン）などの抗ウイルス薬は，ミトコンドリア内のDNAポリメラーゼ活性を阻害するためと考えられている．

2. mtDNAの質的異常：単一欠失/重複，多重欠失

16,600近くある塩基が多数欠失した1種類の環状mtDNAが，正常大のmtDNAと混在して存在するのが単一欠失である[6]．また，欠失したmtDNAと正常大のmtDNAがつながったような大きなmtDNAが検出される場合もある[7]．これが重複（実際は部分重複）である．欠失と重複の検出には，サザン法とPCR法が用いられる．

単一欠失/重複を有するミトコンドリア病の代表は，慢性進行性外眼筋麻痺症候群（chronic progressive external ophthalmoplegia：CPEO），Kearns-Sayre症候群（KSS）であるが，それ以外に乳児期に鉄芽球貧血を含む汎血球減少症，膵外分泌不全を伴うPearson症候群，白質脳症などや老化組織でも検出される（表1）．

欠失の種類が2つ以上ある場合を多重欠失とよんでいる．多重欠失を生じるのは，遺伝性と2次性があり，遺伝性としては常染色体優性遺伝形式の *adenine nucleotide translocator 1* (*ANT1*)[8]，*Twinkle*[9]，*DNA polymarase gamma* (*POLG*)[10]遺伝子の変異が知られており，劣性遺伝形式では *thymidine phosphorylase 1* (*TP1*) 遺伝子変異が報告されている[2]（表1）．また，細胞の崩壊に伴って多重欠失が2次的に起こっていると考えられている病態があり，late-onset mitochondrial myopathyと称される成人発症のミトコンドリアミオパチーのほか，多発性筋炎や筋緊張性筋ジストロフィーでも少量ではあるが多重欠失を認める[11]．

表1　ミトコンドリアDNAの欠乏と欠失を認める病態

欠乏状態	
乳児重症ミオパチー	脳症/筋症
乳児重症肝不全	脳症/肝不全
単一欠失/重複	
Kearns-Sayre症候群	慢性下痢/腸絨毛萎縮
慢性進行性外眼筋麻痺症候群	MELAS
Pearson症候群	ミオパチー/ニューロパチー
Wolfram症候群	尿細管機能障害/糖尿病/小脳失調
失調/白質脳症	その他（多発性筋炎，筋強直性ジストロフィー，老化組織）
糖尿病/難聴	
糖尿病/難聴/黄斑変性/白内障	
多重欠失	
慢性進行性外眼筋麻痺症候群	家族性再発性ミオグロビン尿症
慢性進行性外眼筋麻痺症候群/心筋症	MNGIE
ミオパチー（とくに遅発性）	家族性特発性心筋症
鉄芽球性貧血/ミオパチー	MERRF
進行性脳筋症	

3. リボソームRNA領域の点変異

ミトコンドリア内のリボソームRNA領域の病的変異として，A1555G変異が知られている[12]．これは，アミノグリコシド系抗生物質感受性難聴の患者に認められ，わが国でも比較的頻度が高い．特徴的なことは，高音域から難聴が始まること，1回の投与だけでもその後急速に進行し，高度難聴になること，抗生物質を投与していない人でも難聴をきたすことがあること，などである．アミノグリコシド系抗生物質の投与を行うときには，詳細な問診と場合によってはこの点変異の検査が必要である．

4. 転移RNA領域の点変異

代表的な臨床病型であるMELAS (mitochondrial myopathy, encephalopathy, lactic acidosis and stroke-like episodes) やMERRF (myoclonus epilepsy associated with ragged-red fibers) は，それぞれロイシン (UUR) とリシン転移RNA領域の点変異が病因と認められ，その後数多くの転移RNA領域の点変異が発見された[13,14]（図2）．これらの点変異はほとんどがヘテロプラスミー

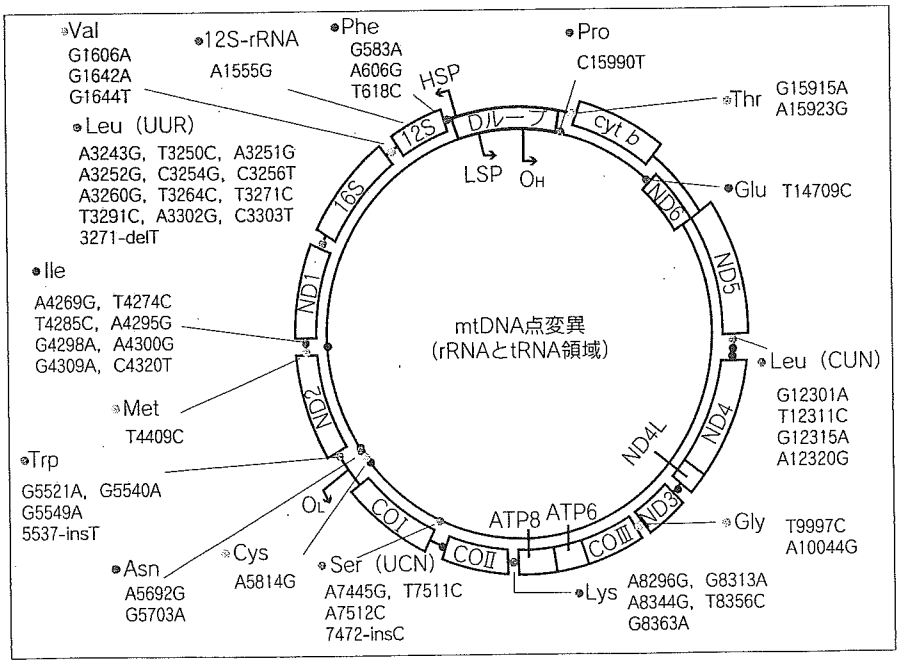

図2　リボソームRNAと転移RNA領域の病的点変異

ミトコンドリアDNAの中で認められた，リボソームRNA (rRNA) 領域と転移RNA (tRNA) 領域の点変異を示す．